Exploring the metabolomic landscape: Perilla frutescens as a promising enhancer of production, flavor, and nutrition in Tan lamb meat

Exploring the metabolomic landscape: *Perilla frutescens* as a promising enhancer of production, flavor, and nutrition in Tan lamb meat

Yue Yu[a], Boyan Zhang[a], Xianzhe Jiang[a], Yimeng Cui[a], Hailing Luo[a], Sokratis Stergiadis[b], Bing Wang[a,*]

[a]*State Key Laboratory of Animal Nutrition and Feeding, College of Animal Science and Technology, China Agricultural University, Beijing 100193, P. R. China*

[b]*University of Reading, School of Agriculture, Policy and Development, Department of Animal Sciences, Reading RG6 6EU, United Kingdom*

*Corresponding author: Bing Wang (wangb@cau.edu.cn)

ABSTRACT

Addressing health-related concerns linked to the metabolite profile of lamb meat has become paramount, in line with the growing demand for enhanced flavor and taste. We examined the impact of *Perilla frutescens* seeds on Tan lamb growth, carcass traits, and metabolite profiles. Three diets were employed: a low-concentrate group (LC), a high-concentrate group (HC), and a PFS group (the LC diet supplemented with 3% *Perilla frutescens* seeds) on a dry matter basis. Forty-five male Tan-lambs (approximately six months) with similar body weights (25.1 kg ± 1.12 SD) were randomly assigned to one of these three groups for 84-day feeding, including an initial 14-day adjustment phase. The supplementation of PFS resulted in increased average daily gain ($P < 0.01$) and improved carcass quality and meat color ($P < 0.05$). Additionally, it led to an enhancement in omega-3 polyunsaturated fatty acids ($P < 0.05$) and a reduction in the omega-6/omega-3 ratio ($P < 0.05$). Using gas chromatography-mass spectrometry, 369 volatile compounds were identified with enhanced levels of acetaldehyde and 1,2,4-trimethyl-benzene associated with PFS ($P < 0.05$). Among the 807 compounds identified by ultra-high performance liquid chromatography-mass spectrometry, there were 66 significantly differential compounds ($P < 0.05$), including 43 hydrophilic metabolites and 23 lipids. PFS supplementation led to significant alterations in 66 metabolites, with three metabolites including 2,5-diisopropyl-3-methylphenol, 3-hydroxydecanoic acid, and lysophosphatidylcholine (15:0) emerging as potential PFS-related biomarkers. The study indicates that PFS supplementation can enhance Tan-lamb growth, feed efficiency, and meat quality, potentially providing lamb meat with improved flavor and nutritional characteristics.

Keywords: fatty acid, volatiles, lipids, lysophosphatidylcholine, flavor and taste precursors

1. Introduction

The cooked meat odor, flavor, and eating taste are closely related to the volatile, lipophilic, and hydrophilic metabolites, and even lipid oxidation compounds in raw meat (Munekata, Pateiro, López-Pedrouso, Gagaoua, & Lorenzo, 2021; Ramalingam, Song, & Hwang, 2019). The lipids and water-soluble compounds are also precursors of these volatile compounds (Khan, Jo, & Tariq, 2015). However, with the development of new techniques and data processing method, liquid chromatography coupled to accurate MS/MS with spectral entropy showed more accurate and helpful for both lipophilic and hydrophilic metabolites and new compounds identification (Li et al., 2021).

Diet is one of the most important factors affecting the flavor metabolites and precursors deposition in raw meat (Khan et al., 2015). The total oil content of *Perilla frutescens* seed can range from 30-45%, of which α-linolenic acid accounts for 50-62% (ALA). Additionally, *Perilla frutescens* seed also contain functional components such as flavonoids, terpenes, polyphenols, amino acids, among others (Akriti, Rajni, & Meenakshi, 2019). In addition, it contains high concentration of essential oils that can act as preservatives in food systems (Al-Maqtari et al., 2022). Consumers nowadays are paying increasing attention to the relationship between food and health (De Smet & Vossen, 2016). Thus, foods enriched with omega-3 PUFAs (n-3 PUFAs) have gained worldwide acclaim, due to their antiviral, anti-inflammatory, immune-boosting and cholesterol-lowering effects (Kavyani et al., 2022), preventing cardiovascular diseases (Sunagawa et al., 2022), and even improving survival in patients with COVID-19 infection (Hathaway et al., 2020). Meanwhile, research indicates that n-3 PUFAs supplementation during pregnancy reduces the risk of developing asthma or asthma symptoms during childhood. Thus, maintaining a moderate intake of n-3 PUFAs is considered crucial for optimal human health.

Despite prior studies on *Perilla frutescens* supplementation (Deng et al., 2018; Peiretti, Gasco, Brugiapaglia, & Gai, 2011) for carcass quality, organoleptic properties, and nutrition in meat, a comprehensive metabolomics analysis of its effect on Tan lamb

metabolism and diverse meat characteristics is lacking. In this study, two integrative untargeted metabolomics approaches were employed to uncover core metabolites and metabolic pathways in Tan sheep, aiming to elucidate the observed phenotypes. We aimed to examine the characteristics related to production (growth rates, feed efficiency), carcass and meat characteristics (classification and basic meat quality parameters), flavour and taste precursors (volatile, lipophilic, and hydrophilic metabolites) and nutritional quality (fatty acid profile, nutritionally-relevant metabolites) of raw meat from lambs fed with *Perilla frutescens* seed.

2. Materials and methods

2.1. Animals, diets, and samples preparation

All animal procedures in the present study were approved by the Animal Care Committee of China Agricultural University (Beijing, China; approval no. AW30901202-1-1). Forty-five male Tan-lambs (*Ovis aries*) (approximately six months of age) with an average bodyweight (BW) of 25.1 kg (± 1.23 SD) were selected on a commercial Tan-sheep farm (Ningxia Hui Autonomous Region, China). The Tan-lambs were randomly divided into three groups with 15 animals in each group (each group has three blocks (pens); each block has five lambs) based on balanced BW using the RAND function in Excel. Each group was allocated in one of the following three experimental treatments: 1) a low-concentrate diet (LC; 45:55 forage: concentrate ratio, on a dry matter (DM) basis); 2) a high-concentrate control diet (HC; 20:80 forage: concentrate ratio, on a DM basis; 3) a LC diet supplemented with 3% *Perilla frutescens* seed (PFS; 3% of diet of Tan-lamb, on a DM basis). The addition of 3% perilla seeds in this study was based a previous study that found the addition of 1% perilla seeds extract of the feed subtract could mitigate the rumen methane production but with no effects on volatile fatty acids (Wang et al., 2016). The detailed ingredients and nutrient composition of the basal diet of are shown in Table 1. *Perilla frutescens* seeds (Purchased from an agricultural food e-commerce) exhibit a nutrient-rich profile with 40.9% ether extract (EE), 23.5% crude protein (CP), 25.4% neutral detergent fiber

(NDF), 19.9% acid detergent fiber (ADF), and 3.9% ash (DM basis). In terms of fatty acids, they contain 57.8% C18:3n3 (ALA), 19.9% C18:1n9c (oleic acid), 11.9% C18:2n6c (linoleic acid), and 7.4% C16:0 (palmitic acid, % of total fatty acids) (Table 2). The diets were fed as total mixed ration and the *Perilla frutescens* seed was uniformly mixed into the concentrates. The offered feed and refusals from each pen were weighed and recorded daily to determine the DM intake. The lambs were fed twice a day at 09:00 and 17:00. All the lambs had ad libitum access to feed and water throughout the experimental period. The experiment lasted for 84 d, including a 14 d adaptation period, plus 70 d of the feeding experiment.

An untargeted metabolomics was conducted for the botanical bioactive compounds for PFS based on the LC-MS/MS analysis, which was performed on an UHPLC system (Vanquish, Thermo Fisher Scientific) with a Waters UPLC BEH C18 column (1.7 μm 2.1*100 mm). The detail protocol was following a previous study (Hou et al., 2019).

2.2. Carcass traits, basic meat quality and targeted fatty acid analysis

At the end of the feeding experiment (on the d 70), 6 lambs per group (2 lambs from each pen) were randomly selected for slaughter. The selection was performed using the RAND function in Excel. Slaughter was conducted following the outlined procedure: euthanasia; skinning; removal of the head at the atlas-occipital joint; cutting of the limbs at the carpo-metacarpal and tarso-metatarsal joints; removal of the heart, liver, spleen, lungs, kidneys, and testis; excision of the omental, perirenal, and tail fat deposits. The organs and carcass weights were measured and recorded immediately after slaughtering, and the organs' index were calculated based on their ratio to carcass weight. Immediately after slaughtering, the body fat (assessed as GR value) and loin-eye area were measured. The GR value was determined by using a vernier caliper to measure the thickness at the $12^{th}/13^{th}$ rib intersection, 11 cm away from the midline (Karim, Porwal, Kumar, & Singh, 2007). The loin-eye area was determined using a planimeter (QCJ-2000, Harbin Optical Instrument Factory, Harbin, China) at the interface of 12^{th} and 13^{th} ribs on both sides of the carcass (Karim, Porwal, Kumar, &

Singh, 2007). Then, meat samples taken from the 6th to 12th ribs of the left *longissimus lumborum* (LL) muscle were trimmed of fat. The determination of pH and meat colour were performed between 12th and 13th thoracic vertebrae. To measure the pH values of LL muscle samples at 45 min and 24 h postmortem, a pH meter with automatic temperature compensation was used after calibration with pH 4.6 and 7.0 buffers. Meat color parameters such as redness (a^*), yellowness (b^*), and lightness (L^*) were measured in triplicate after 30 min of blooming at room temperature (approximately at 20 °C) using an NS800 high-quality spectrophotometer (3NH Technology co., Ltd, Shenzhen, China). The measurements were conducted at 45 min and 24 h after slaughter, using illuminant D65 as the light source and a 10° observer with an 8 mm diameter measuring area and a 50 mm diameter illumination area (Honikel, 1998). The LL (from the 6th to 12th ribs) at 24 h post-mortem was used to assess instrumental meat quality characteristics including cooking rate and shear force (Ekiz et al., 2009). After thawing at 4 °C, the meat was cut into rectangular 2 × 2 × 1 cm samples weighing approximately 30 ± 1 g and the connective tissue was removed. The muscle samples were placed in plastic vacuum packs (two steaming batch) and placed in a water bath at 75 °C for approximately 30 min until the final core temperature reached 70 °C. The samples were then cooled to room temperature, the surface of the samples was dried with paper towels, and cooking rate was measured and calculated as follows: (Weight of the samples after cooking / Weight of the samples before cooking) × 100%. After measuring the cooking rate, three sub-samples (cut parallel to the muscle fibres and 1 × 1 cm in cross-section) were removed from each cooked sample. Shearing perpendicular to the muscle fiber direction was performed using a TMS-PRO Texture Analyzer (FTC Co., Ltd., Virginia, USA) equipped with a WBSF (Warner-Bratzler Shear Force) device featuring a 250 Newton load cell, employing an across-head speed of 60 mm/min.

The LL samples from the 12th/13th rib at 45 min were collected to freezing tubes and stored in liquid nitrogen for further metabolomics study. The LL samples taken from the 6th to 12th rib section at 24 h postmortem were stored in dry ice and then were used for targeted fatty acid composition via gas chromatography (Model 6890; Agilent Technologies, Santa Clara, CA, USA) equipped with a DB-23 capillary column (60.0

m×250 μm×0.25 μm) following our previous method (Zhang et al., 2022). The standard sample mixture (F.A.M.E. Mix, C4-C24 Unsaturates, Supelco-18919-1AMP, Sigma-Aldrich Trading Co.Ltd., Shanghai, China), which consisted of 40 free fatty acids, was used in the analysis. C11:0 (1.0 mg/mL) was employed as the internal standard. The fatty acid results expressed as mg/100 g of wet meat samples. The following combinations and ratios of fatty acids were calculated: saturated fatty acids (SFA), unsaturated fatty acids (UFA), total fatty acids (TFA), monounsaturated fatty acids (MUFA), conjugated linoleic acid (CLA), PUFA, SFA/UFA, and omega-6/omega-3 ratio (n-6/n-3). The index of atherogenicity (IA) = (C12:0 + (4 × C14:0) + C16:0) / (MUFA + PUFA), and index of thrombogenicity index (IT) = (C14:0 + C16:0 + C18:0) / (0.5 × MUFA) + (0.5 × n-6) + (3×n-3) + (n-3:n-6) were calculated based on a previous study (Pretorius & Schonfeldt, 2021).

2.3. Volatile compounds identification based on GC-MS analysis

A 300 ± 5 mg LL sample was transferred into a 20 mL headspace vial, to which 10 μL of a 2-octanol internal standard (at a concentration of 10 mg/L in deionized water) was added. Subsequent analysis was conducted using a gas chromatography-mass spectrometry (GC-MS) system, specifically during the Solid Phase Microextraction (SPME) cycle of the PAL rail system. The sample incubation temperature was set to 60 °C, with a preheating duration of 15 min, followed by an incubation period of 30 min. The desorption time was 4 min. The GC-MS analysis was performed on an Agilent 7890 gas chromatograph system coupled with a 5977B mass spectrometer, utilizing a DB-Wax column. The sample was injected in splitless mode. Helium served as the carrier gas, with a front inlet purge flow of 3 mL/min and a column gas flow rate of 1 mL/min. The initial oven temperature was set to 40 °C and maintained for 4 min, then incrementally increased to 245 °C at a rate of 5 °C/min, where it was held for an additional 5 min. The temperatures for the injection port, transfer line, ion source, and quadrupole were set at 250 °C, 250 °C, 230 °C, and 150 °C, respectively. Ionization was achieved using an energy of -70 eV in electron impact mode. Mass spectrometry

data acquisition was performed in scan mode, covering a mass-to-charge ratio (m/z) range of 20-400, with no solvent delay. Raw peak extraction, baseline data filtering and calibration, peak alignment, deconvolution analysis, peak identification, integration, and spectral matching of peak areas were conducted utilizing the Chroma TOF 4.3X software developed by LECO Corporation in conjunction with the NIST database (Garcia & Barbas, 2011).

2.4. Higher definition mix discovery metabolomics based on LC-MS/MS analysis

Twenty-five mg of the LL sample was accurately weighed and transferred into a polypropylene microcentrifuge tube. Subsequently, 500 μL of an extraction solution, composed of methanol and water in a 3:1 ratio with an isotopically-labelled internal standard mixture (250 nmol/L), was added to the sample. The samples underwent a homogenization process at a frequency of 35 Hz for a duration of 4 min, followed by a 5-min sonication in an ice-water bath. This homogenization and sonication cycle was conducted thrice. Post these cycles, the samples were subjected to an incubation period of 1 hour at a temperature of -40 ℃, followed by centrifugation at a rotational speed of 13,800 *g* for 15 min at 4 ℃. The supernatant resulting from the centrifugation was carefully transferred into a new, clean glass vial for further analysis. A quality control (QC) sample was prepared by amalgamating equal aliquots of supernatants from all samples.

The analytical assessments were conducted utilizing a high-definition (HD) mix Ultra-High-Performance Liquid Chromatography (UHPLC) system (Vanquish, Thermo Fisher Scientific) integrated with a UPLC HSS T3 column (2.1 mm × 100 mm, 1.8 μm), linked to an Orbitrap Exploris 120 mass spectrometer (Orbitrap MS, Thermo) (UHPLC-OE-MS). The mobile phase comprised of 5 mmol/L ammonium acetate and 5 mmol/L acetic acid in water (A), alongside acetonitrile (B). The autosampler was maintained at a temperature of 4 ℃, with an injection volume of 2 μL. The Orbitrap Exploris 120 mass spectrometer was employed due to its capacity for acquiring MS/MS spectra using information-dependent acquisition (IDA) mode under the supervision of the Xcalibur

acquisition software (Thermo). In this specified mode, the software incessantly assesses the complete scan MS spectrum. The ESI source conditions were preordained as follows: sheath gas flow rate at 50 Arb, auxiliary gas flow rate at 15 Arb, capillary temperature at 320 ℃, full MS resolution at 60,000, MS/MS resolution at 15,000, collision energy at 10/30/60 in Normalized Collision Energy (NCE) mode, and spray voltage at 3.8 kV (positive) or -3.4 kV (negative). The raw data was converted into mzXML format utilizing ProteoWizard and subsequently processed with an in-house developed program, founded on XCMS. This program facilitated peak detection, extraction, alignment, and integration. Post-processing, an in-house MS2 database (BiotreeDB, V2.1) was utilized for metabolite annotation, with an annotation cut-off established at 0.3.

2.5. Statistical analysis

Variation in animal growth performance, carcass traits, meat quality, and targeted fatty acid analysis were described using linear mixed models by the IBM SPSS Statistics (version 26.0), with three treatments (LC, HC, and PFS) as a fixed effect and random terms for animal and pen. Predicted means and standard errors were obtained from the models, facilitating pairwise comparisons between means by calculating the least significant difference at a 5% critical value. The value of $P < 0.05$ was considered statistically significant.

For the data from GC-MS and LC-MS/MS, the missing values were assumed to be half of the minimum value (Tiedt et al., 2020). Normalisation was implemented using the total ion current method. The consolidated dataset, inclusive of peak number, sample identifiers, and normalised peak areas, was transferred to the SIMCA16.0.2 software package (Sartorius Stedim Data Analytics AB, Umea, Sweden) for comprehensive multivariate analyses. Data were scaled and logarithmically transformed to attenuate the influence of both background noise and significant variance across variables. Post-transformation, principal component analysis (PCA) was implemented as an unsupervised analytic method to condense the dimensionality

of the dataset, providing visual interpretation of sample distribution and clustering. A 95% confidence interval within the PCA score plot was utilized as the criterion for potential outlier identification. Supervised orthogonal projections to latent structures-discriminant analysis (OPLS-DA) was employed for visualizing group differentiation and the identification of significantly altered metabolites. The validity and predictability of the model were assessed by executing a 7-fold cross-validation, yielding R^2 and Q^2 values. R^2 quantifies the extent to which variation in a variable is elucidated, whereas Q^2 denotes the predictability of a variable. The robustness and predictive capability of the OPLS-DA model were verified via a 200-iteration permutation test, from which the intercept values for R^2 and Q^2 were ascertained. In this context, a smaller Q^2 intercept value is indicative of a robust model with low risk of overfitting and high reliability. The value of variable importance in the projection (VIP) of the first principal component in OPLS-DA analysis was obtained. It summarizes the contribution of each variable to the model. The metabolites with VIP > 1 and $P < 0.05$ (student t test) were considered as significantly changed metabolites. In addition, commercial databases including KEGG (http://www.genome.jp/kegg/) and MetaboAnalyst (http://www.metaboanalyst.ca/) were used for pathway enrichment analysis.

3. Results

3.1. The plant secondary metabolites of PFS

The top 5 catteries of the plant secondary metabolites of PFS are flavonoids (37%), phenylpropanoids (28%), terpenoids (11%), quinones (11%), alkaloid (11%, Fig. S1A). For the specific compounds, luteolin (22%), 7-hydroxycoumarin (15%), and emodin (9%) are the most abundant bioactive compounds (Fig. S1B).

3.2. Growth performance and carcass characteristics

As shown in Table 3, there was no significant effect of the dietary treatments on dry matter intake (DMI) ($P > 0.05$). The HC exhibited the highest average daily gain (ADG, 194 g/d), followed by PFS (154 g/d), with LC (120 g/d) presenting the lowest value ($P < 0.01$). The feed conversion rate (average DMI/ADG) was lower in HC (4.78) than in LC (8.28, $P < 0.05$). The carcass traits, including live weight, carcass weight, and dressing percentage of HC and PFS, were higher than those of LC ($P < 0.05$), with no significant differences observed between HC and PFS. The HC had the higher head weight compared to LC (2.72 kg vs 2.42 kg, $P < 0.05$). The organ weight of the heart was higher in HC (145 g) and PFS (136 g) than in LC (120 g), with similar values between HC and PFS ($P < 0.01$). The organ weights of the kidney in HC (101.2 g) were higher than those in LC (41.4 g) and PFS (46.2 g), with similar values between LC and PFS ($P < 0.01$). The organ ratio of the heart was higher in LC than in PFS (8.52 vs 7.87 g/kg carcass weight, $P < 0.05$). The organ ratios of the lung and testis were higher in LC (21.2 and 22.4 g/kg carcass weight) than in HC (16.8 and 19.8 g/kg carcass weight) and PFS (16.6 and 18.3 g/kg carcass weight, $P < 0.01$). The organ ratios of the kidney were higher in HC (5.62 g/kg carcass weight) than in LC (2.95 g/kg carcass weight) and PFS (2.65 g/kg carcass weight, $P < 0.01$).

3.3. Meat quality

As shown in Table 4, the tail fat weight and the tail fat ratio were higher in HC than in LC ($P < 0.05$). The perirenal fat weight and perirenal fat ratio were highest in the HC group, followed by PFS, with the lowest value found in LC ($P < 0.01$). The omentum weight and omentum ratio were higher in HC and PFS than in LC ($P < 0.01$). The eye muscle area was greater in HC than in LC ($P < 0.05$). The value of shear force was higher in LC than in HC ($P < 0.05$). The meat color of a^* (redness) after 24 hours was lower in PFS than in HC ($P < 0.05$).

3.4. Targeted fatty acids composition

The raw meat DM content, intramuscular fat (IMF) content, and fatty acid profiles

in muscle are displayed in Table 5. The DM content in PFS was higher than in LC ($P < 0.01$). The HC had higher levels of C10:0, C16:1, and TFA compared to LC ($P < 0.05$). Compared to LC, the concentrations of C22:0 and C23:0 were lower, but the concentrations of UFA, MUFA, and C18:1c9 were higher in LC and PFS ($P < 0.05$). The PFS had higher concentration of C20:0 but lower C20:3n6 compared to LC. The PFS exhibited higher concentrations of α-linolenic acid (C18:3n3, ALA), C20:5n3 (eicosapentaenoic, EPA), C22:6n3 (docosahexaenoic acid, DHA) and the sum of n-3 PUFA compared to LC and HC ($P < 0.05$). Compared to PFS and LC, HC had higher levels of CLA-t10c12, C18:2n6, and the sum of n-6 PUFA ($P < 0.05$). The SFA/UFA ratio was lower in HC and PFS than in LC ($P < 0.01$). The ratio of n-6/n-3 was lowest in PFS (8.02), intermediate in LC (15.2), and highest in HC (21.3, $P < 0.01$). The values of IA, IT, and C16:0/C18:1 were lower in PFS and HC than in LC ($P < 0.05$).

3.5. Volatile compounds

In this experiment, a total of 434 peaks were detected, and 421 metabolites remained after relative standard deviation denoising based on GC-MS analysis. According to the HMDB and Biotree self-built databases, 369 of these metabolites were identified and categorized into 6 groups (Fig. 1A). The 6 categories are alcohols, aldehydes, ketones, esters, hydrocarbons, and others. Alcohols were the most abundant VOCs (Fig. 1A).A multivariate statistical analysis of volatile compounds (VOCs) was performed. The OPLS-DA revealed a clear separation of volatile compounds between the two groups (R^2X= 0.26, R^2Y=0.95, Q^2=0.0703, Fig. 1B). The permutation plot and histogram test of the OPLS-DA model suggest that the original OPLS-DA model did not exhibit overfitting, indicating a relatively robust model (Fig. S2A-B).

Eight compounds were significantly different between these two groups, with 2,4-dihydroxybenzoic acid, 1,2,4-trimethylbenzene, and acetaldehyde being up-regulated by the PFS, and pyridine, 2-butanol, dl-isocitric acid lactone, 3,3-dimethylbutane-2-ol, and 4-ethylcyclohexanone down-regulated by the PFS (Fig. 1C). Meanwhile, 2,4-dihydroxybenzoic acid (AUC = 0.94), 3,3-dimethylbutane-2-ol (AUC = 0.94), and 4-

ethyl-cyclohexanone (AUC = 0.97) were selected as the potential VOCs biomarker to distinguish PFS from CON (Fig. 1D).

3.6. High definition mix discovery LC-MS/MS metabolome

Based on the high definition (HD) mix UHPLC-OE-MS discovery metabolomics, both hydrophilic substances and lipophilic metabolites can be detected. A total of 22,630 peaks were detected in this experiment, and 17,985 peaks were retained after relative standard deviation de-noising. The Fig. S2C shows the score chart based on PCA analysis; all samples are located in the 95% confidence interval. The OPLS-DA model showed an apparent group separation between the two groups (R^2X= 0.215, R^2Y=1, Q^2=0.275, Fig. S2D) and the model is robust based on permutations and interceptions (Fig. S2E-F). According to the HMDB database and self-built database, a total of 422 hydrophilic metabolites were identified, belonging to various categories: organic acids and derivatives (25.1%); organoheterocyclic compounds (20.38%); phenylpropanoids and polyketides (13.03%); organic oxygen compounds (12.32%); benzenoids (10.9%); nucleosides, nucleotides, and analogues (7.35%); organic nitrogen compounds (4.03%); alkaloids and derivatives (1.18%); organosulfur compounds (0.71%); homogeneous non-metal compounds (0.47%); lignans, neolignans and related compounds (0.47%); hydrocarbons (0.24%); organic compounds (0.24%); organohalogen compounds (0.24%); and others (3.32%) (Fig. 2A). A total of 385 lipids were identified, belonging to various classes: phosphatidylcholine (PC, 16.88%); acyl carnitine (AcCa, 11.69%); free fatty acid (FFA, 10.91%); lysophosphatidylcholine (LPC, 5.45%); lysophosphatidylethanolamine (LPE, 3.12%); phosphatidylglycerol (PG, 2.86%); phosphatidylinositol (PI, 2.34%); phosphatidylethanolamine (PE, 2.08%); sphingomyelin (SM, 1.82%); ceramides (Cer, 0.78%); phosphatidylserine (PS, 0.26%); triglycerides (TG, 0.26%); Coenzyme (Co, 0.26%); and others (41.30%) (Fig. 2B). Among these lipids categories, the LPC in PFS was lower than that in LC, and Co was higher in PFS than that in LC (Fig. 2C).

In total, 66 compounds were screened out as significantly different metabolites by HD mix LC-MS/MS (VIP > 1, $P < 0.05$). Among the hydrophilic metabolites, 43 compounds showed statistically significant differences (Fig. 2D). These included the upregulated macrophorin A, hydroxyprolyl-Isoleucine, sedoheptulose, rotenone, D-pantothenic acid, 5-hydroxyisourate, D-glutamine, xanthylic acid, S-adenosyl-L-methionine, uridine diphosphate glucuronic acid, 5'-inosinic acid, inosine 2'-phosphate, arginyl-alanine, aromadendrin, 3-ethyl-5-methylphenol, 2,5-diisopropyl-3-methylphenol, and N-desmethylvenlafaxine, and downregulated guanidinosuccinic acid, L-norleucine, 3,4-dihydroxybenzaldehyde, 1,6-dimethoxypyrene, tectorigenin, 2,4-dimethyloxazole, macrocarpal I, nornicotine, 3-hydroxydecanoic acid, L-valine, adrenosterone, pelargonic acid, 2-hydroxybutyric acid, gyromitrin, guanosine-5'-triphosphate, 7-aminoflunitrazepam, zedoarondiol, 2-methylbutyroylcarnitine, and fexofenadine by PFS compared to LC. In lipids, there are 23 substances with different lipid molecular species affected by PFS (Fig. 2E). In the PFS group, one species of AcCa, one species of Co, one species of PC, and two species of PG significantly increased. Conversely, nine species of LPC, one species of LPE, and eight species of PC decreased (Fig. 2E). Meanwhile, 2,5-diisopropyl-3-methylphenol (AUC = 1), 3-hydroxydecanoic acid (AUC = 1), and LPC(15:0) (AUC = 1) were the potential PFS related biomarker in lamb meat based on ROC analysis (Fig. 2F).

3.7. Metabolic pathways analysis

Based on the KEGG enrichment analysis (Fig. 3A), we found the pathways of purine metabolism and choline metabolism in cancer were enriched ($P < 0.05$). On the other hand, the metabolic pathways contributing to the metabolite differences of lamb meat were also conducted based on MetaboAnalyst (Fig. 3B). The bubble plot showed that the differential metabolites were mainly enriched in the ascorbate and aldarate metabolism, valine, leucine and isoleucine biosynthesis, pentose and glucuronate interconversions, and propanoate metabolism.

4. Discussion

4.1. Growth performance and carcass characteristics

Previous study found no significant improvement in the growth rate and carcass traits after the inclusion of 5%, 10% or 15% perilla seed in the diet, on a DM basis, of Hu-lambs (Deng et al., 2018). In this study, the HC diet, which has the highest dietary metabolic energy level, was set as a positive control. The results from the HC group indicated that the lambs fed with a higher energy diet exhibited increased growth performance but also higher fat deposition. The PFS significantly increased carcass weight and dressing percentage in Tan sheep compared to LC, which was similar to the carcass characteristics in HC. This improvement could be partly attributed to increased energy intake in the PFS group compared to the LC group, in line with previous observations that a higher growth rate can be achieved through oil supplementation in goats and sheep (Candyrine et al., 2018). In addition, feeding PFS increased the DM content of raw meat while reducing meat redness. Myoglobin interacts with oxygen to form the bright red oxymyoglobin, which along with myoglobin can be oxidized to the brown-colored high-iron content metmyoglobin, consequently affecting the perceived redness of the tissue (Brewer, 2004). Flavonoids, known to prevent the production of free radicals (Zhu et al., 2022), are enriched in *Perilla* seeds in our study. Consequently, the PFS might increase the activity of myoglobin reductase and delay the oxidation of myoglobin, potentially reducing meat redness when PFS was fed to lambs. The enhanced growth performance, increased carcass yield, and altered meat color observed in the PFS-fed group may be attributed to both the energy content of PFS and the presence of functional plant secondary metabolites. Thus, supplementing PFS in lamb diets, can synergistically improve the growth performance and carcass quality of lamb, when compared with diets with low concentrates; although the growth rates achieved by a HC diet would still be higher than a PFS diet.

4.2. Meat fatty acid profiles

This study mainly found that the PFS could increase the lamb meat UFA and n-3 PUFA content and reduced the n-6/n-3, IA, and IT. The lamb fed with HC diet had

higher n-6 PUFA content which result in the highest n-6/n-3. The accumulation of n-3 and n-6 PUFA in lamb meat are through direct consumption from diets or via desaturation and elongation processes from short-chain fatty acid precursors (Ponnampalam, Sinclair, & Holman, 2021). Hence, the elevated levels of n-6 PUFA in lamb meat from the HC group can be attributed to the common derivation of short-chain n-6 PUFA from grain-based and feedlot diets. The SFA may enhance lipid adhesion to immunological and circulatory system cells (pro-atherogenic), while UFA could inhibit plaque formation and reduce certain lipid levels, thereby decreasing the risk of coronary diseases (anti-atherogenic) (FAO, 2010). The firmness of adipose tissue is contingent upon the degree of fatty acid saturation, a factor that plays a critical role in determining the nutritional merit of meat products and their subsequent acceptance by consumers (Wood et al., 2004). It has been reported that n-3 PUFAs have properties that improve antioxidant capacity and nutritional value of meat, as well as playing a crucial role in health maintenance (Sunagawa et al., 2022). The diet's primary significant sources of preformed long-chain PUFAs such as eicosapentaenoic acid (C20:5 n3) and docosahexaenoic acid (C22:6 n3) are derived exclusively from ruminant meats and oily fish (Wyness et al., 2011). The consumption of lamb meat with reduced levels of n-6 PUFA and increased levels of n-3 PUFA had the potential to enhance both animal and human health, well-being, and resilience against diseases (Ponnampalam et al., 2021). The present study found higher concentrations of total n-3 PUFAs (+ 64%), C20:5n3 (+ 49%), and C18:3n3 (+ 83%) in PFS compared to LC, thus demonstrating a nutritionally improved fatty acid profile (Wood et al., 2004). Diet plays a pivotal role in shaping the fatty acid composition of lamb fat (Wood et al., 2004). Notably, the choice of dietary oil source can significantly impact the fatty acid content in lamb meat (Jeronimo, Alves, Prates, Santos-Silva, & Bessa, 2009). Furthermore, the presence of plant flavonoids has been shown to modify the fatty acid profiles of lamb meat (North, Dalle Zotte, & Hoffman, 2019). Thus, the reduction of SFA/UFA, n-6/n-3 PUFA, IA, and IT in the raw lamb meat from PFS group might be mainly explained by the high content of PUFA and plant flavonoids, and the production of PFS lamb meat can further

be regarded as beneficial effects from a public health and human nutrition perspective (Pretorius & Schonfeldt, 2021).

4.3. Compounds contribute to meat flavour and human health

The VOCs and their respective precursors substantially influence the olfactory characteristic of ovine meat, or mutton, wherein the resultant odor profile is a complex interplay governed by their relative concentrations and perceptual thresholds (Zhan, Tian, Zhang, & Wang, 2013). Aldehydes typically possess a relatively low odor threshold, and as a result, they are regarded as having a vital impact on the distinct flavor of lamb meat (Zhang, Zhang, Liu, Zhao, & Luo, 2020), primarily originating from PUFAs (Hu et al., 2022). In this research, aldehyde serves as the primary aromatic active compounds based on VOC analysis. Acetaldehyde and acetal are types of aldehydes that have a fruity odor with sweet and astringent notes and play a role in forming the primary liquor aroma by assisting other flavor compounds (Wei, Zou, Shen, & Yang, 2020). 1,2,4-Trimethyl-benzene is thermal degradation product of β-carotene, which is produced in high amounts in the orange flesh color, imparting strong violet aromas (Wang & Kays, 2003). In addition, the pelargonic acid, an oily liquid with an unpleasant, rancid odor (Liu et al., 2022), was found to be decreased by PFS using HD mix LC-MS. 5'-lnosinic acid, identified as a taste-active component in the chicken meat extract (Fujimura et al., 1996), suggests that the taste of PFS lamb meat might be improved by increasing its 5'-inosinic acid content. Therefore, the changes in VOCs and related hydrophilic metabolites in lamb meat suggest that feeding PFS may enhance the aroma, flavor, and taste of raw lamb.

In addition, aroma compounds are mainly formed by lipids (Munekata et al., 2021). Thus, the lipids were further detected by a HD mix UHPLC-OE-MS. Compared with normal LC-MS, HD LC-MS/MS has a mixed hydrophilic and lipophilic system, specifically the T3 chromatographic system, which can enhance the resolution and reliability in MS-oriented characterization of hydrophilic and lipophilic metabolites (Ding et al., 2022). Lipid subclasses (SM, Cer, LPC, PC, LPE, TG) in Tan sheep meat

458 can be significantly influenced by thermal processing (Jia, Li, Wu, Liu, & Shi, 2021).
459 We found the total LPC, 9 species of LPC, 7 species of PC, and 1 species of LPE were
460 decreased by PFS, and 2 species of PG were increased by PFS. LPC(15:0) was also the
461 potential biomarker to discriminate PFS from LC by the ROC analysis. LPC(15:0) was
462 used to predict inflammatory response to TNF-α inhibitors in rheumatoid arthritis
463 (Cuppen et al., 2016). In hepatic inflammation, there is a notable elevation in the
464 concentrations of LPC and LPE, with particularly LPC as a potential biomarker in the
465 diagnosis and monitoring of hepatic steatosis (Engel, Schiller, Galuska, & Fuchs, 2021).
466 The addition of PG(18:1/18:1) and PG(18:2/18:2) can effectively reduce mitochondrial
467 inflammation (Chen, Chao, Chang, Chan, & Hsu, 2018). Thus, the decreased LPC and
468 increased PG(18:1/18:1) and PG(18:1/18:2) indicate the potentially desirable
469 nutritional and safety characteristics of PFS lamb meat for consumers.

470 Furthermore, most of the potential detrimental hydrophilic metabolites were
471 reduced by feeding PFS. For instance, the PFS reduced the relative abundance of
472 muscular guanidinosuccinic acid that has been identified as a uraemic toxin (Duranton
473 et al., 2012), and the hepatic guanidinosuccinic acid can be elevated in lambs under a
474 high-energy diet induced immune response (Wang et al., 2023). 3-hydroxydecanoic
475 acid is a potential negative biomarker associated with PFS. The tissue accumulation of
476 3-hydroxydecanoic acid is associated with increased disease risk such as
477 cardiomyopathy (Tonin et al., 2013). 2-Methylbutyroylcarnitine is an acylcarnitine, a
478 group of compounds gaining recognition as crucial markers in metabolic investigations
479 of various illnesses, such as metabolic disorders, cardiovascular diseases, diabetes,
480 depression, neurological disorders, and some types of cancer (Dambrova et al., 2022).
481 Thus, another potential benefit to human nutrition by consuming meat from lambs fed
482 with PFS is the reduced concentrations of these compounds which are associated to
483 various diseases.

484 Conversely, several metabolites that underwent substantial changes or potential
485 biomarkers associated with PUFAs in lamb meat have yet to be thoroughly researched.
486 Even though 2,5-diisopropyl-3-methylphenol was identified in the current investigation
487 as a potential biomarker of PUFA-enhanced lamb meat, further investigations are

required to corroborate its association with PUFAs, understand its role in lamb physiology, and determine its impact on human nutrition and health.

5. Conclusions

The present study demonstrated that the dietary inclusion of *Perilla frutescens* seeds improved growth performance and simultaneously improved carcass quality and raw meat attributes in Tan-lambs. An increased n-3 PUFAs content and a decrease in the n-6/n-3, IA, and IT were observed in raw lamb meat as a result of feeding PFS. These changes are considered nutritionally desirable. Volatile compounds, including acetaldehyde and 1,2,4-trimethyl-benzene, were found in higher concentrations in PFS, which suggests an improved flavor profile for PFS raw lamb meat. In addition, several nutritionally beneficial lipids and hydrophilic metabolites were associated with PFS treatment, including PG(18:1/18:1), PG(18:2/18:2), and 5'-inosinic acid. Metabolites such as LPC, guanidinosuccinic acid, 3-hydroxydecanoic acid, and 2-methylbutyroylcarnitine, known to exert negative impacts on human health, were found in lower concentrations in PFS raw lamb meat. The present findings provide exhaustive understanding of the metabolome of raw lamb meat with improved n-3 PUFAs and corresponding volatile, lipidic, and hydrophilic metabolites achieved through the incorporation of *Perilla frutescens* seed. Additionally, the global alteration of compounds detected through HD-mix LC-MS/MS metabolomics proposes its utility as a replacement for lipidomics and hydrophilic metabolomics.

Funding

This study was funded by the Open Project of the Key Laboratory of Molecular Animal Nutrition, Ministry of Education (KLMAN202206) and China Agriculture Research System (No. CARS-38). We greatly acknowledge the personnel of Tianyuan Liangzhong Sheep Farm (Wuzhong, China) for their help in animal feeding.

CRediT authorship contribution statement

Yue Yu: Writing - original draft, Formal analysis. **Boyan Zhang:** Writing - review & editing, Resources, Conceptualization. **Xianzhe Jiang**: Writing - review & editing. **Yimeng Cui**: Investigation. **Hailing Luo**: Writing - review & editing, Resources. **Sokratis Stergiadis**: Writing - review & editing. **Bing Wang**: Project administration, Writing - review & editing, Supervision, Conceptualization.

Declaration of Competing Interest

The authors declare no conflict of interest.

Data availability

Data will be made available on request.

References

Akriti, D., Rajni, C., & Meenakshi, G. (2019). A review on nutritional value, functional properties and pharmacological application of Perilla (Perilla Frutescens L.). *Biomedical & Pharmacology Journal, 12*(2), 649-660.

Al-Maqtari, Q. A., Rehman, A., Mahdi, A. A., Al-Ansi, W., Wei, M., Yanyu, Z., . . . Yao, W. (2022). Application of essential oils as preservatives in food systems: challenges and future prospectives – a review. *Phytochemistry Reviews, 21*(4), 1209-1246.

Brewer, S. (2004). Irradiation effects on meat color - a review. *Meat Science, 68*(1), 1-17.

Candyrine, S. C. L., Jahromi, M. F., Ebrahimi, M., Chen, W. L., Rezaei, S., Goh, Y. M., . . . Liang, J. B. (2018). Oil supplementation improved growth and diet digestibility in goats and sheep fed fattening diet. *Asian-Australasian Journal of Animal Sciences, 32*(4), 533-540.

Chen, W.-W., Chao, Y.-J., Chang, W.-H., Chan, J.-F., & Hsu, Y.-H. H. (2018). Phosphatidylglycerol incorporates into cardiolipin to improve mitochondrial activity and inhibits inflammation. *Scientific Reports, 8*(1), 1-14.

Cuppen, B. V., Fu, J., van Wietmarschen, H. A., Harms, A. C., Koval, S., Marijnissen, A. C., . . . all Society for Rheumatology Research Utrecht Investigators. (2016). Exploring the inflammatory metabolomic profile to predict response to TNF-alpha inhibitors in Rheumatoid Arthritis. *PLoS One, 11*(9), e0163087.

Dambrova, M., Makrecka-Kuka, M., Kuka, J., Vilskersts, R., Nordberg, D., Attwood, M. M., . . . Schioth, H. B. (2022). Acylcarnitines: nomenclature, biomarkers, therapeutic potential, drug targets, and clinical trials. *Pharmacol Reviews, 74*(3), 506-551.

De Smet, S., & Vossen, E. (2016). Meat: The balance between nutrition and health. A review. *Meat Science, 120*, 145-156.

Deng, K. P., Fan, Y. X., Ma, T. W., Wang, Z., TanTai, W. J., Nie, H. T., . . . Wang, F. (2018). Carcass traits, meat quality, antioxidant status and antioxidant gene expression in muscle and liver of Hu lambs fed perilla seed. *Journal of Animal Physiology and Animal Nutrition, 102*(2), e828-e837.

549 Ding, X., Liu, Z., Liu, Y., Xu, B., Chen, J., Pu, J., . . . Wang, X. (2022). Comprehensive evaluation of the
550 mechanism of Gastrodia elata Blume in ameliorating cerebral ischemia-reperfusion injury based
551 on integrating fecal metabonomics and 16S rDNA sequencing. *Frontiers in Cellular and*
552 *Infection Microbiology, 12*, 1026627.
553 Duranton, F., Cohen, G., De Smet, R., Rodriguez, M., Jankowski, J., Vanholder, R., & Argiles, A. (2012).
554 Normal and pathologic concentrations of uremic toxins. *Journal of the American Society of*
555 *Nephrology, 23*(7), 1258-1270.
556 Ekiz, B., Yilmaz, A., Ozcan, M., Kaptan, C., Hanoglu, H., Erdogan, I., & Yalcintan, H. (2009). Carcass
557 measurements and meat quality of Turkish Merino, Ramlic, Kivircik, Chios and Imroz lambs
558 raised under an intensive production system. *Meat Science, 82*(1), 64-70.
559 Engel, K. M., Schiller, J., Galuska, C. E., & Fuchs, B. (2021). Phospholipases and reactive oxygen
560 species derived lipid biomarkers in healthy and diseased humans and animals - a focus on
561 lysophosphatidylcholine. *Frontiers in Physiology, 12*, 732319.
562 FAO. (2010). Fats and fatty acids in human nutrition. Report of an expert consultation. *FAO Food and*
563 *Nutrition Paper, 91*, 1-166.
564 Fujimura, S., Koga, H., Takeda, H., Tone, N., Kadowaki, M., & Ishibashi, T. (1996). Role of taste-active
565 components, glutamic acid, 5'-inosinic acid and potassium ion in taste of chicken meat extract.
566 *Animal Science and Technology, 67*(5), 423-429.
567 Garcia, A., & Barbas, C. (2011). Gas chromatography-mass spectrometry (GC-MS)-based metabolomics.
568 *Methods in Molecular Biology, 708*, 191-204.
569 Hathaway, D., Pandav, K., Patel, M., Riva-Moscoso, A., Singh, B. M., Patel, A., Abreu, R. (2020). Omega
570 3 fatty acids and COVID-19: a comprehensive review. *Infection and Chemotherapy, 52*(4), 478-
571 495.
572 Honikel, K. O. (1998). Reference methods for the assessment of physical characteristics of meat. *Meat*
573 *Science, 49*(4), 447-457.
574 Hou, J. J., Zhang, J. Q., Yao, C. L., Bauer, R., Khan, I. A., Wu, W. Y., & Guo, D. A. (2019). Deeper
575 chemical perceptions for better traditional Chinese medicine standards. *Engineering, 5*(1), 83-
576 97.
577 Hu, Y., Zhao, G., Yin, F., Liu, Z., Wang, J., Qin, L., . . . Zhu, B. (2022). Effects of roasting temperature
578 and time on aldehyde formation derived from lipid oxidation in scallop (Patinopecten yessoensis)
579 and the deterrent effect by antioxidants of bamboo leaves. *Food Chemistry, 369*, 130936.
580 Jeronimo, E., Alves, S. P., Prates, J. A., Santos-Silva, J., & Bessa, R. J. (2009). Effect of dietary
581 replacement of sunflower oil with linseed oil on intramuscular fatty acids of lamb meat. *Meat*
582 *Science, 83*(3), 499-505.
583 Jia, W., Li, R., Wu, X., Liu, S., & Shi, L. (2021). UHPLC-Q-Orbitrap HRMS-based quantitative
584 lipidomics reveals the chemical changes of phospholipids during thermal processing methods
585 of Tan sheep meat. *Food Chemistry, 360*, 130153.
586 Karim, S. A., Porwal, K., Kumar, S., & Singh, V. K. (2007). Carcass traits of Kheri lambs maintained on
587 different system of feeding management. *Meat Science, 76*(3), 395-401.
588 Kavyani, Z., Musazadeh, V., Fathi, S., Hossein Faghfouri, A., Dehghan, P., & Sarmadi, B. (2022).
589 Efficacy of the omega-3 fatty acids supplementation on inflammatory biomarkers: An umbrella
590 meta-analysis. *International Immunopharmacology, 111*, 109104.
591 Khan, M. I., Jo, C., & Tariq, M. R. (2015). Meat flavor precursors and factors influencing flavor
592 precursors--A systematic review. *Meat Science, 110*, 278-284.

Li, Y., Kind, T., Folz, J., Vaniya, A., Mehta, S. S., & Fiehn, O. (2021). Spectral entropy outperforms MS/MS dot product similarity for small-molecule compound identification. *Nature Methods, 18*(12), 1524-1531.

Liu, Z., Xu, L., Song, P., Wu, C., Xu, B., Li, Z., & Chao, Z. (2022). Comprehensive quality evaluation for medicinal and edible Ziziphi Spinosae semen before and after rancidity based on traditional sensory, physicochemical characteristics, and volatile compounds. *Foods, 11*(15), 2320.

Munekata, P. E. S., Pateiro, M., López-Pedrouso, M., Gagaoua, M., & Lorenzo, J. M. (2021). Foodomics in meat quality. *Current Opinion in Food Science, 38*, 79-85.

North, M. K., Dalle Zotte, A., & Hoffman, L. C. (2019). The use of dietary flavonoids in meat production: A review. *Animal Feed Science and Technology, 257*, 114291.

Peiretti, P. G., Gasco, L., Brugiapaglia, A., & Gai, F. (2011). Effects of perilla (Perilla frutescens L.) seeds supplementation on performance, carcass characteristics, meat quality and fatty acid composition of rabbits. *Livestock Science, 138*(1-3), 118-124.

Ponnampalam, E. N., Sinclair, A. J., & Holman, B. W. B. (2021). The sources, synthesis and biological actions of omega-3 and omega-6 fatty acids in red meat: An overview. *Foods, 10*(6), 1358.

Pretorius, B., & Schonfeldt, H. C. (2021). Cholesterol, fatty acids profile and the indices of atherogenicity and thrombogenicity of raw lamb and mutton offal. *Food Chemistry, 345*, 128868.

Ramalingam, V., Song, Z., & Hwang, I. (2019). The potential role of secondary metabolites in modulating the flavor and taste of the meat. *Food Research International, 122*, 174-182.

Sunagawa, Y., Katayama, A., Funamoto, M., Shimizu, K., Shimizu, S., Sari, N., . . . Morimoto, T. (2022). The polyunsaturated fatty acids, EPA and DHA, ameliorate myocardial infarction-induced heart failure by inhibiting p300-HAT activity in rats. *The Journal of Nutritional Biochemistry, 106*, 109031.

Tiedt, S., Brandmaier, S., Kollmeier, H., Duering, M., Artati, A., Adamski, J., . . . Dichgans, M. (2020). Circulating metabolites differentiate acute ischemic stroke from stroke mimics. *Annals of Neurology, 88*(4), 736-746.

Tonin, A. M., Amaral, A. U., Busanello, E. N., Grings, M., Castilho, R. F., & Wajner, M. (2013). Long-chain 3-hydroxy fatty acids accumulating in long-chain 3-hydroxyacyl-CoA dehydrogenase and mitochondrial trifunctional protein deficiencies uncouple oxidative phosphorylation in heart mitochondria. *Journal of Bioenergetics and Biomembranes, 45*(1-2), 47-57.

Wang, B., Zhang, B., Zhou, L., Li, S., Li, Z., & Luo, H. (2023). Multi-omics reveals diet-induced metabolic disorders and liver inflammation via microbiota-gut-liver axis. *The Journal of Nutritional Biochemistry, 111*, 109183.

Wang, J., Liu, M., Wu, Y., Wang, L., Liu, J., Jiang, L., & Yu, Z. (2016). Medicinal herbs as a potential strategy to decrease methane production by rumen microbiota: a systematic evaluation with a focus on Perilla frutescens seed extract. *Applied Microbiology and Biotechnology, 100*(22), 9757-9771.

Wang, Y., & Kays, S. J. (2003). Analytically directed flavor selection in breeding food crops. *Journal of the American Society for Horticultural Science, 128*(5), 711-720.

Wei, Y., Zou, W., Shen, C. H., & Yang, J. G. (2020). Basic flavor types and component characteristics of Chinese traditional liquors: A review. *Journal of Food Science, 85*(12), 4096-4107.

Wood, J. D., Richardson, R. I., Nute, G. R., Fisher, A. V., Campo, M. M., Kasapidou, E., . . . Enser, M. (2004). Effects of fatty acids on meat quality: a review. *Meat Science, 66*(1), 21-32.

Wyness, L., Weichselbaum, E., O'connor, A., Williams, E., Benelam, B., Riley, H., & Stanner, S. (2011).

637 Red meat in the diet: an update. *Nutrition Bulletin, 36*(1), 34-77.
638 Zhan, P., Tian, H., Zhang, X., & Wang, L. (2013). Contribution to aroma characteristics of mutton process
639 flavor from the enzymatic hydrolysate of sheep bone protein assessed by descriptive sensory
640 analysis and gas chromatography olfactometry. *Journal of Chromatography B-Analytical*
641 *Technologies in the Biomedical and Life Sciences, 921-922*, 1-8.
642 Zhang, B., Sun, Z., Yu, Z., Li, H., Luo, H., & Wang, B. (2022). Transcriptome and targeted metabolome
643 analysis provide insights into bile acids' new roles and mechanisms on fat deposition and meat
644 quality in lamb. *Food Research International, 162*, 111941.
645 Zhang, C., Zhang, H., Liu, M., Zhao, X., & Luo, H. (2020). Effect of breed on the volatile compound
646 precursors and odor profile attributes of lamb meat. *Foods, 9*(9), 1178.
647 Zhu, W., Han, M., Bu, Y., Li, X., Yi, S., Xu, Y., & Li, J. (2022). Plant polyphenols regulating myoglobin
648 oxidation and color stability in red meat and certain fish: A review. *Critical Reviews in Food*
649 *Science and Nutrition*, 1-13.
650

651 **Tables**

652 **Table 1**

653 Ingredients and nutrient composition of the basal diet.

Item	LC[1]	HC[1]
Ingredient, % dry matter basis		
Corn grain	26.40	48.00
Soybean meal	12.80	14.20
Wheat bran	11.10	12.80
Corn silage	9.00	13.20
Alfalfa Hay	16.00	6.80
Caragana microphylla silage	20.00	0.00
$NaHCO_3$	0.70	1.00
Perilla frutescens seed	0.00	0.00
Premix[2]	4.00	4.00
Nutrients		
Metabolic energy, MJ/kg	10.01	11.22
Crude protein, %	14.27	14.27
Neutral detergent fiber, %	37.84	22.39
Acid detergent fiber, %	24.56	11.16
Non-fiber carbohydrate, %	34.09	50.57
Ether extract, %	4.10	5.41
Ash, %	6.30	3.25
Calcium, %	0.81	0.51
Phosphorus, %	0.40	0.46

654 [1]LC: low-concentrate diet; HC: high-concentrate diet

655 [2]Formulated to provide (per kilogram of dry matter): 500,000 IU of vitamin A, 160,000
656 IU of vitamin D3, 650 IU of vitamin E, 150 g of NaCl, 20 g of Ca, 20 g of P, 1750 mg
657 of Zn, 15 mg of Se, 50 mg of I, 2000 mg of Fe, 20 mg of Co, 1500 mg of Mn, and 600
658 mg of Cu.

Table 2

The nutrient composition and fatty acid profiles of *Perilla frutescens* seeds (dry matter basis).

Item	Composition	
Nutrients		
Crude protein, %		22.03
Neutral detergent fiber, %		23.82
Acid detergent fiber, %		18.67
Non-fiber carbohydrate, %		12.12
Ether extract, %		38.39
Ash, %		3.64
Fatty acids	mg/100g	% of total fatty acids
C8:0	3.48	0.01
C12:0	1.90	0.01
C14:0	8.19	0.03
C15:0	3.24	0.01
C16:0	2337	7.38
C16:1	32.55	0.10
C17:0	2.32	0.01
C18:0	698.45	2.20
C18:1n9c	6312	19.94
C18:2n6c	3767	11.90
C18:3n3	18292	57.78
C20:0	69.25	0.22
C20:1	55.91	0.18
C21:0	9.84	0.03
C20:2	8.18	0.03
C20:4n6	11.90	0.04
C22:0	17.54	0.06
C22:1n9	10.88	0.03
C24:0	17.10	0.05
Total fatty acids	31658	100.00

Table 3

The growth performance and carcass characteristics of Tan-lamb

Items	Treatments[1]			SEM	*P*-value
	LC	HC	PFS		
Growth performance					
Initial BW, kg	25.4	25.0	25.3	0.30	0.674
DMI, g/d	934	961	869	41.0	0.345
ADG, g/d	120c	194a	157b	11.9	<0.001
FCR	8.28a	4.78b	5.44ab	1.848	0.061
Carcass traits					
Live weight, kg	31.1b	37.0a	35.4a	0.67	<0.001
Carcass weight, kg	14.1b	18.0a	17.3a	0.29	<0.001
Dressing percentage, %	45.6b	49.0a	48.8a	0.59	0.001
Head weight, kg	2.42b	2.72a	2.57ab	0.069	0.026
Hooves weight, kg	0.63	0.79	0.73	0.013	0.292
Pelage weight, kg	2.45	3.50	2.82	0.197	0.078
GR	6.03	7.98	6.99	1.020	0.458
The organ weight, g					
Heart	120b	145a	136a	3.7	0.001
Liver	507	660	523	33.8	0.083
Spleen	56.0	62.0	59.0	9.99	0.913
Lung	299	304	287	17.2	0.545
Kidney	41.4b	101.2a	46.2b	2.75	<0.001
Testis	316	358	315	13.6	0.100
The organ ratio, g/kg of carcass weight					
Heart	8.52a	8.07ab	7.87b	0.197	0.089
Liver	35.8	36.3	30.4	1.80	0.098
Spleen	3.79	3.36	3.54	0.522	0.842
Lung	21.2a	16.8b	16.6b	0.68	0.001
Kidney	2.95b	5.62a	2.65b	0.119	<0.001
Testis	22.4a	19.8b	18.3b	0.76	0.016

[a-c] Means within a row with different subscripts differ when *P*-value < 0.05.

[1] LC, low-concentrate diet; HC, high-concentrate diet; PFS: 3% *Perilla frutescens* seed supplementation in LC; BW, body weight; DMI, dry matter intake; ADG, average daily gain; FCR, feed conversion ratio (DMI/ADG); GR, the depth of muscle and fat tissue from the surface of the carcass to the lateral surface of the 12th rib 110mm from the midline.

671 **Table 4**

672 The fat distribution and raw meat quality of Tan-lamb

Items	Treatments[1]			SEM	*P*-value
	LC	HC	PFS		
Fat distribution					
Tail fat, g	1098b	1979a	1546ab	145.3	0.019
Tail fat ratio, g/kg	77.6b	110a	89.1ab	8.33	0.079
Perirenal fat, g	35c	287a	141b	26.4	<0.001
Perirenal fat ratio, g/kg	2.5c	15.9a	8.1b	1.50	<0.001
Omentum, g	154b	270a	322a	21.3	0.001
Omentum ratio, g/kg	10.9b	14.8a	18.7a	1.19	0.006
Meat quality					
Eye muscle area, cm^2	15.6b	18.4a	17.7ab	0.89	0.098
Cooking rate, %	59.1	59.2	61.0	1.06	0.350
Shear force, *N*	63.7	47.0	52.2	5.00	0.081
pH 45 min	6.73	6.58	6.62	0.078	0.392
*a** 45 min	8.5	8.3	9.0	0.45	0.519
*b** 45 min	7.6	7.3	7.6	0.31	0.695
*L** 45 min	34.3	34.2	34.2	0.69	0.987
pH 24 h	5.76	5.76	5.92	0.074	0.249
*a** 24 h	12.0a	10.7ab	10.2b	0.49	0.050
*b** 24 h	10.7	12.4	10.5	1.28	0.425
*L** 24 h	38.1	41.5	38.1	0.70	0.106

673 [a-c] Means within a row with different subscripts differ when *P*-value < 0.05.

674 [1] LC, low-concentrate diet; HC, high-concentrate diet; PFS: 3% *Perilla frutescens* seed

675 supplementation in LC; *a**, redness; *b**, yellowness; *L**, lightness.

676 **Table 5**

677 The fatty acid composition (mg/100g tissue, wet fresh matter basis) and health index

678 in the raw meat of Tan-lamb

	Treatments[1]				
Items	LC	HC	PFS	SEM	*P*-value
DM content of raw meat, %	22.9b	24.7a	25.9a	0.56	0.009
IMF, % FM	1.85	2.80	2.38	0.316	0.138
IMF, % DM	8.08	11.2	9.37	1.247	0.239
ΣSFA	879	1137	1128	128	0.152
C10:0	2.51b	3.57a	3.44ab	0.522	0.090
C12:0	3.30	3.12	3.82	0.896	0.570
C14:0	47.9	51.2	60.5	12.95	0.338
C15:0	7.02	9.71	7.24	1.894	0.294
C16:0	424	577	569	75.7	0.116
C17:0	20.9b	40.7a	21.3b	5.54	0.033
C18:0	346	427	429	35.0	0.187
C20:0	3.12b	3.44ab	3.93a	0.221	0.057
C21:0	11.6	10.0	11.4	1.23	0.200
C22:0	2.77a	2.19b	1.99b	0.231	0.005
C23:0	2.84a	2.11b	2.34b	0.275	0.011
C24:0	2.82	2.45	2.70	0.161	0.278
ΣUFA	916b	1310a	1271a	137.8	0.041
ΣMUFA	701b	1051a	1043a	126.3	0.037
C14:1	1.79	2.02	2.42	0.585	0.251
C16:1	27.8b	41.1a	39.1ab	6.19	0.074
C18:1c9	666b	1003a	996a	119.1	0.035
C20:1	2.54	2.41	2.45	0.263	0.939
C22:1n9	1.07	0.99	0.98	0.096	0.762
C24:1	2.87	2.53	2.52	0.184	0.334
ΣPUFA	207	252	218	15.3	0.121
CLA-c9t11	3.96	3.96	3.75	0.308	0.865
CLA-t10c12	1.16b	1.73a	1.13b	0.307	0.035
Σn-3	13.6b	11.5b	25.4a	1.51	<0.001
C18:3n3	7.53b	6.49b	15.7a	1.007	<0.001
C20:5n3	3.27b	2.67b	5.44a	0.415	<0.001
C22:6n3	2.61b	2.44b	3.96a	0.411	0.012
Σn-6	194b	241a	194b	14.5	0.053
C18:2n6	126b	171a	132b	11.6	0.028
C20:3n6	5.37a	4.79ab	4.53b	0.461	0.098
C20:4n6	61.9	64.4	57.2	3.04	0.262
ΣTFA	1795b	2447a	2399ab	265.3	0.077
SFA/UFA	0.96a	0.87b	0.88b	0.018	0.003
MUFA/PUFA	3.45	4.25	4.54	0.397	0.139
n-6/n-3	15.2b	21.3a	8.02c	1.127	<0.001

C16:0/C18:1	0.64a	0.58b	0.56b	0.012	0.001
IA	0.68a	0.60b	0.62b	0.017	0.020
IT	1.68a	1.56b	1.51b	0.039	0.017

679 [a-b] Means within a row with different subscripts differ when *P*-value < 0.05.

680 [1] LC, low-concentrate diet; HC, high-concentrate diet; PFS: 3% *Perilla frutescens* seed
681 supplementation in LC; DM, dry matter; FM, fresh matter; IMF, intramuscular fat; SFA,
682 saturated fatty acids; UFA, unsaturated fatty acids; MUFA, monounsaturated fatty acids;
683 PUFA, polyunsaturated fatty acids; CLA, conjugated linoleic acid; TFA, total fatty
684 acids; IA, index of atherogenicity; IT, index of thrombogenicity.

FIGURE CAPTIONS

Fig. 1. The profiles of volatile compounds (VOCs) in *longissimus lumborum* based on GC-MS. (A) The relative proportion of volatile categories in the two groups. (B) Principal component analysis (PCA) score plots of volatile compounds. (C) The volcano plot and differential VOCs between LC and PFS. (D) Biomarker analysis results of VOCs (ROC curve view).

Fig. 2. The profiles of lipids and hydrophilic metabolites in *longissimus lumborum* based on high definition mix LC-MS. (A) Percentages of categories of lipids and hydrophilic metabolites. (B) Percentages of numbers of lipid species. (C) Difference in lipid species between LC and PFS lamb. (D) Significant different hydrophilic molecular. (E) Significant different lipids molecular. (F) Biomarker analysis results of HD mix LC-MS metabolomics (ROC curve view). *Represents significant differences using Student's two-tailed t-test. (*$P < 0.05$). AcCa, acyl carnitine; Cer, ceramides; Co, coenzyme; FFA, free fatty acid; LPC, lysophosphatidylcholine; LPE, lysophosphatidylethanolamine; PC, phosphatidylcholine; PE, phosphatidylethanolamine; PG, phosphatidylglycerol; PI, phosphatidylinositol; PS, phosphatidylserine; SM, sphingomyelin; TG, triglyceride.

Fig. 3. The enriched metabolic pathways and co-occurrence network analyses of the different volatile, lipophilic, and hydrophilic metabolites. (A) Metabolic pathways (top 15) according to KEGG enrichment analysis of different metabolites (B) Overview of pathway analysis of significant metabolites using Metaboanalyst 5.0.

A

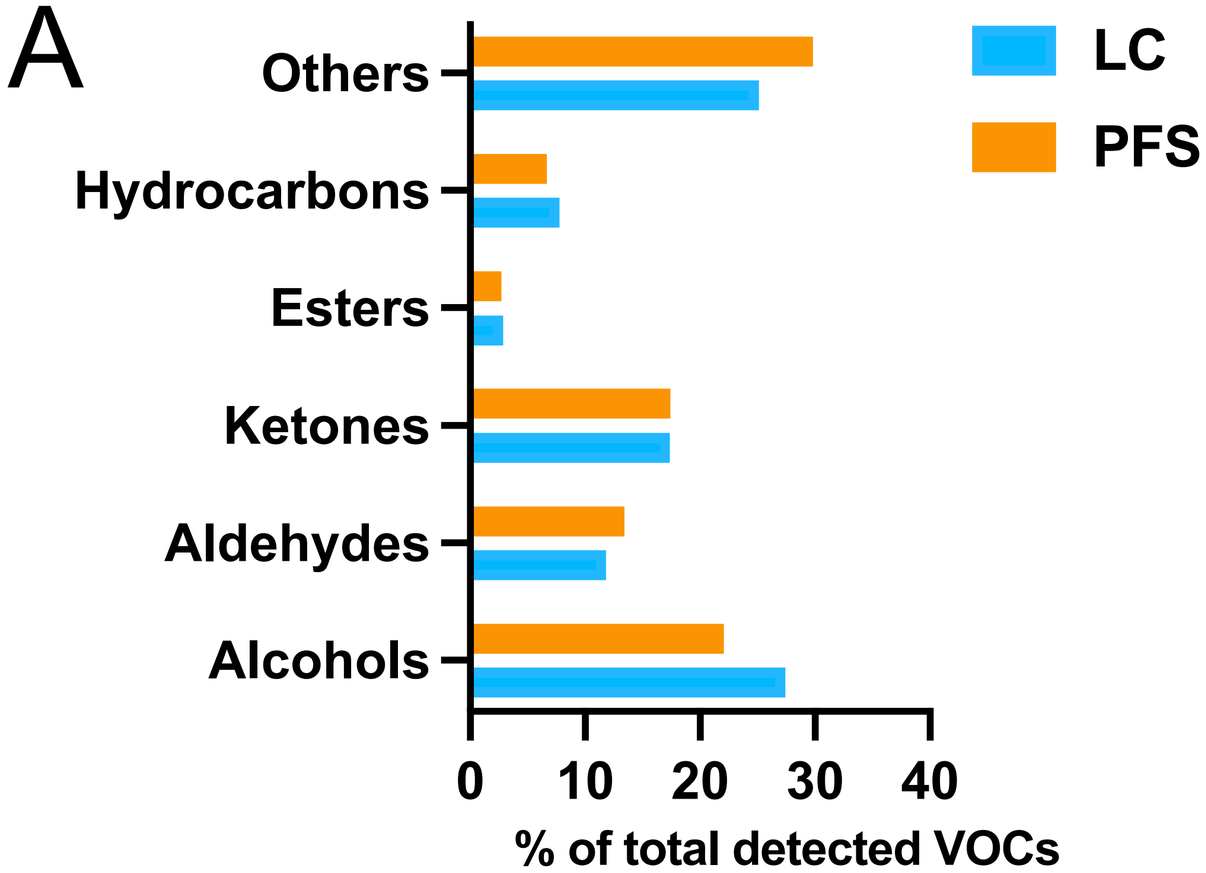
Others
Hydrocarbons
Esters
Ketones
Aldehydes
Alcohols
LC
PFS
0
10
20
30
40
% of total detected VOCs

B

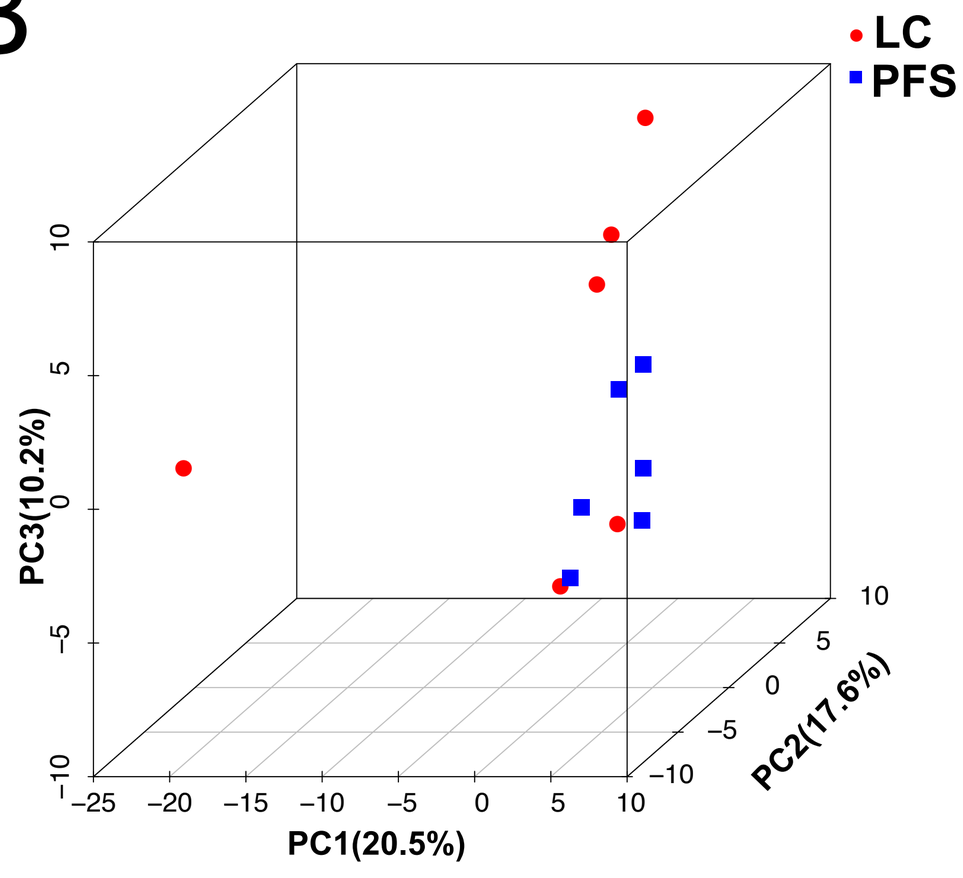
LC
PFS
PC3(10.2%)
PC1(20.5%)
PC2(17.6%)

C

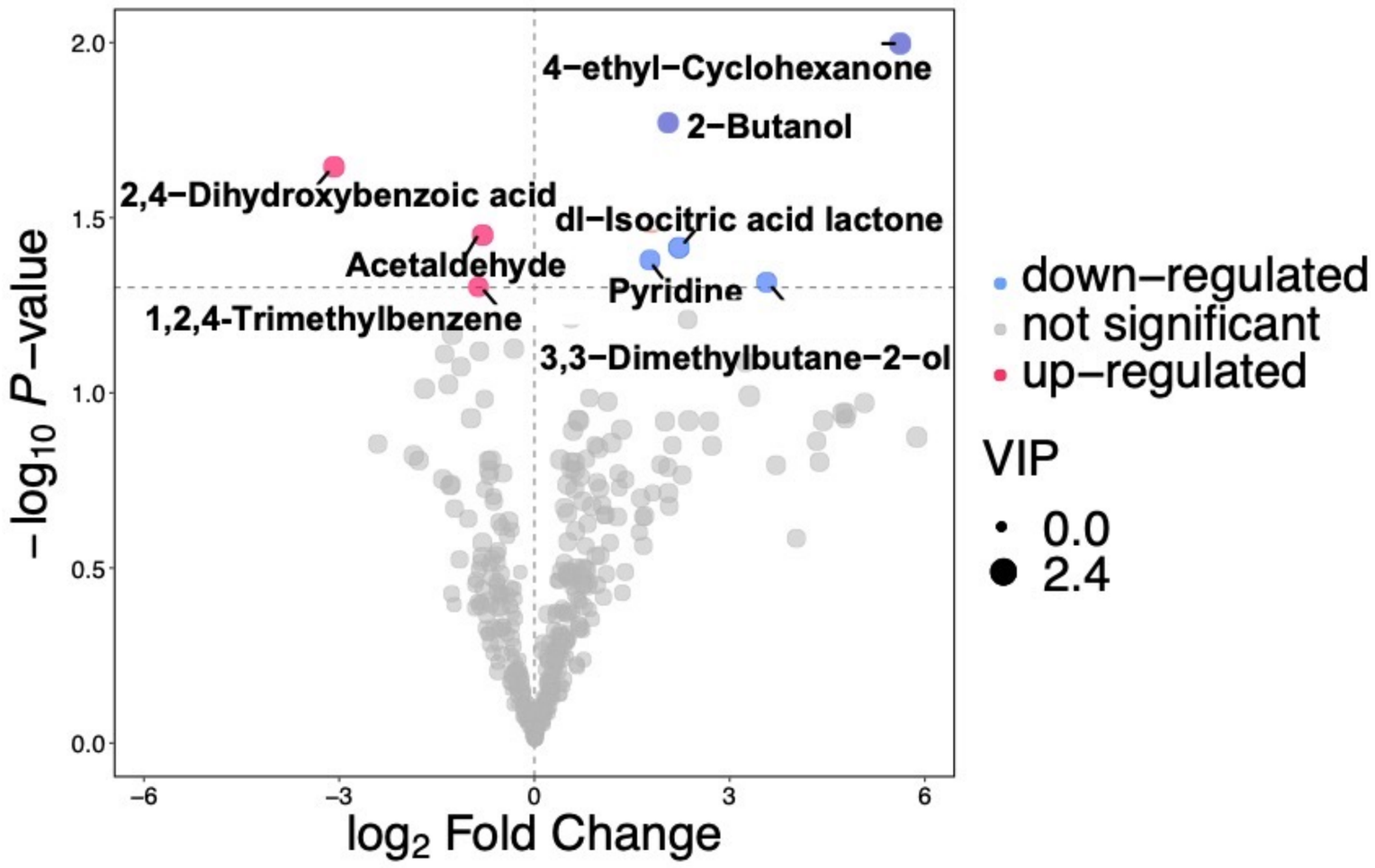
4−ethyl−Cyclohexanone
2−Butanol
2,4−Dihydroxybenzoic acid
dl−Isocitric acid lactone
Acetaldehyde
Pyridine
1,2,4-Trimethylbenzene
3,3−Dimethylbutane−2−ol
down−regulated
not significant
up−regulated
VIP
0.0
2.4
−log10 P−value
log2 Fold Change

D

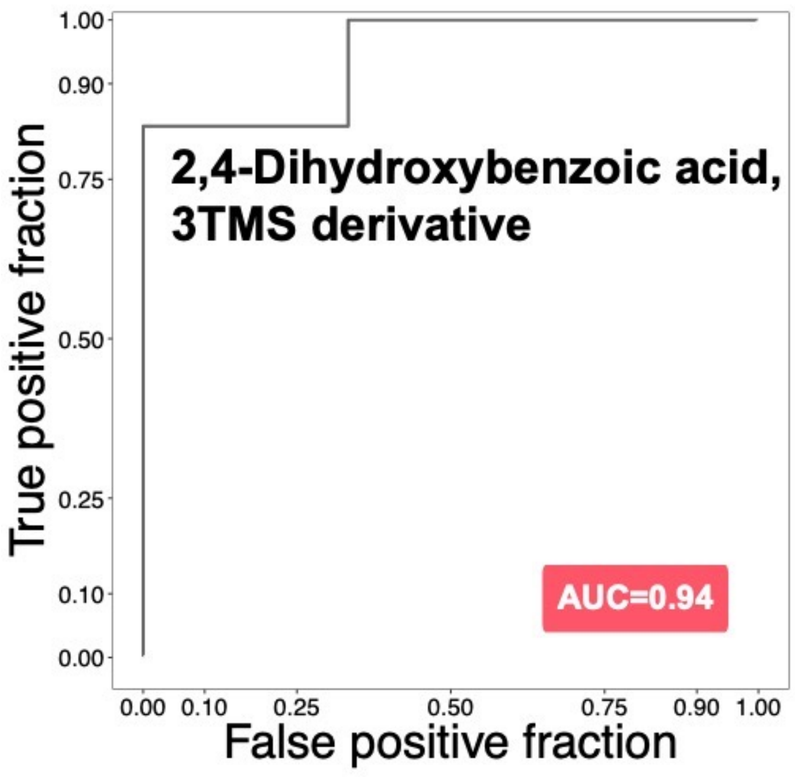
2,4-Dihydroxybenzoic acid, 3TMS derivative
AUC=0.94
True positive fraction
False positive fraction

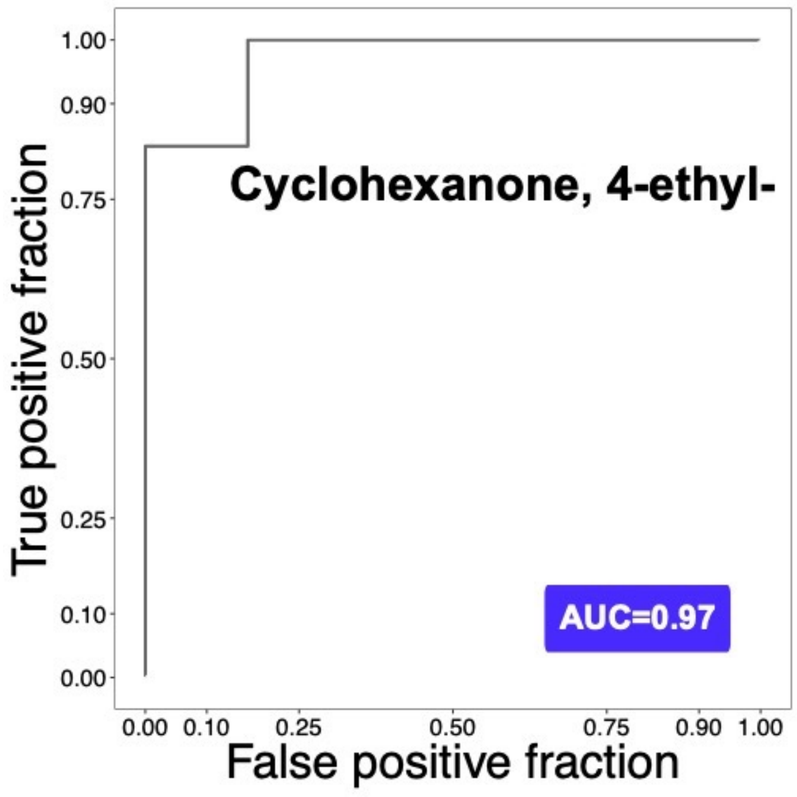
Cyclohexanone, 4-ethyl-
AUC=0.97
True positive fraction
False positive fraction

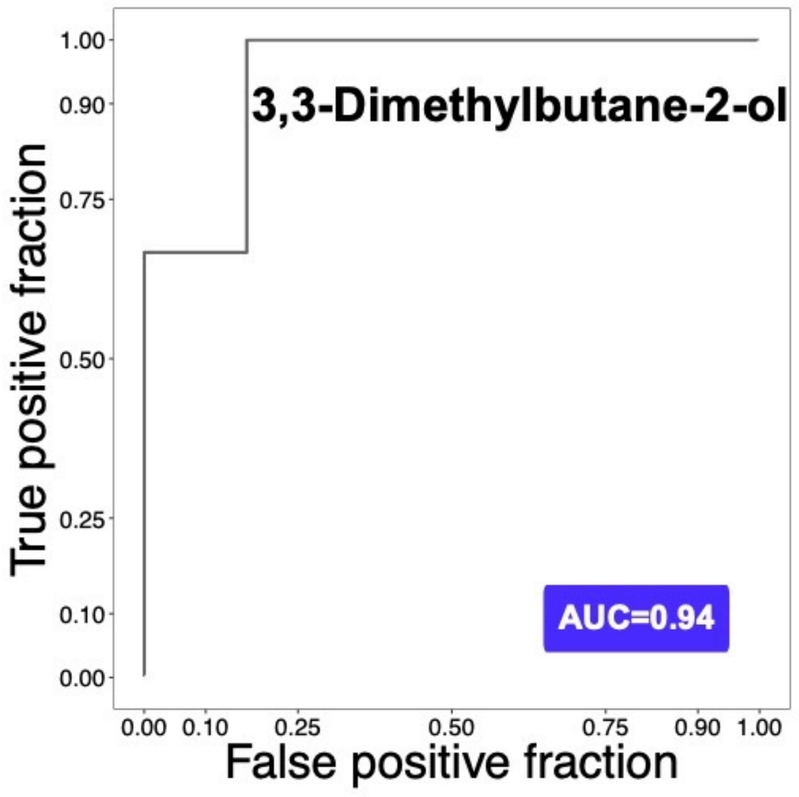
3,3-Dimethylbutane-2-ol
AUC=0.94
True positive fraction
False positive fraction

A

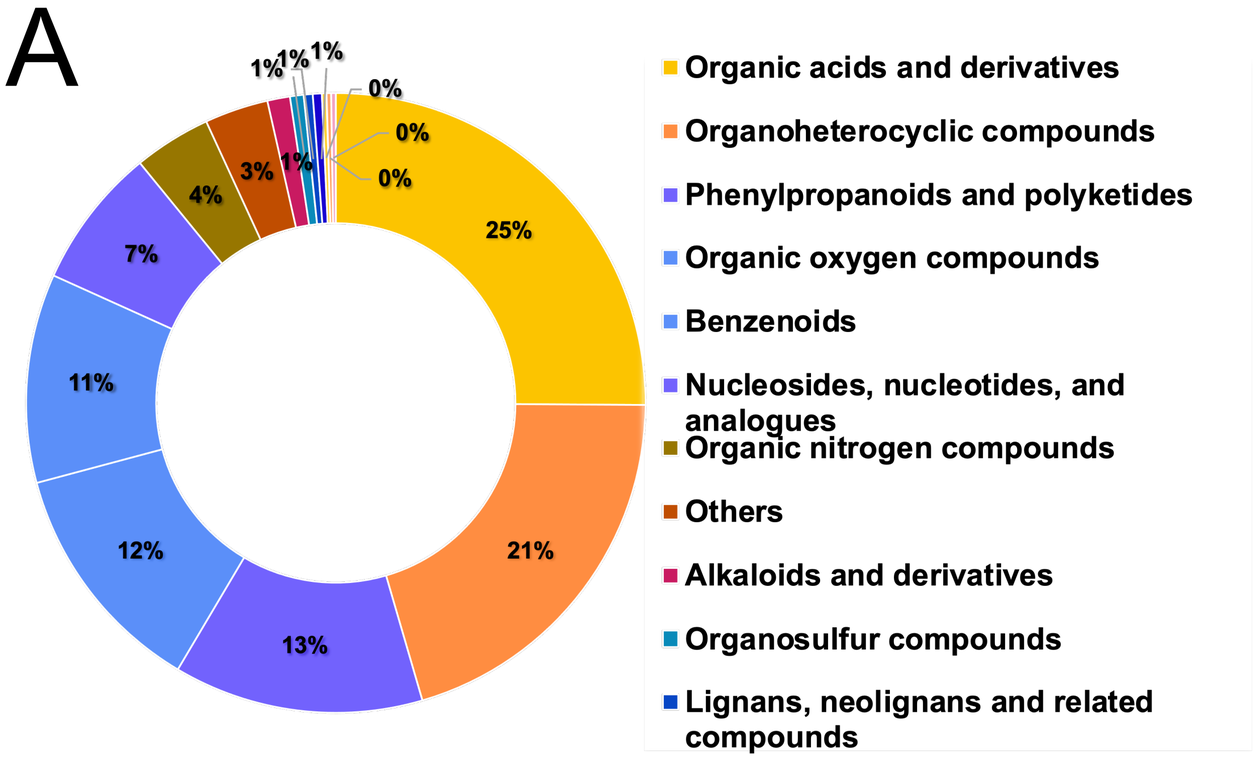
25%
21%
13%
12%
11%
7%
4%
3%
1%
1%
1%
1%
0%
0%
0%
Organic acids and derivatives
Organoheterocyclic compounds
Phenylpropanoids and polyketides
Organic oxygen compounds
Benzenoids
Nucleosides, nucleotides, and analogues
Organic nitrogen compounds
Others
Alkaloids and derivatives
Organosulfur compounds
Lignans, neolignans and related compounds

B

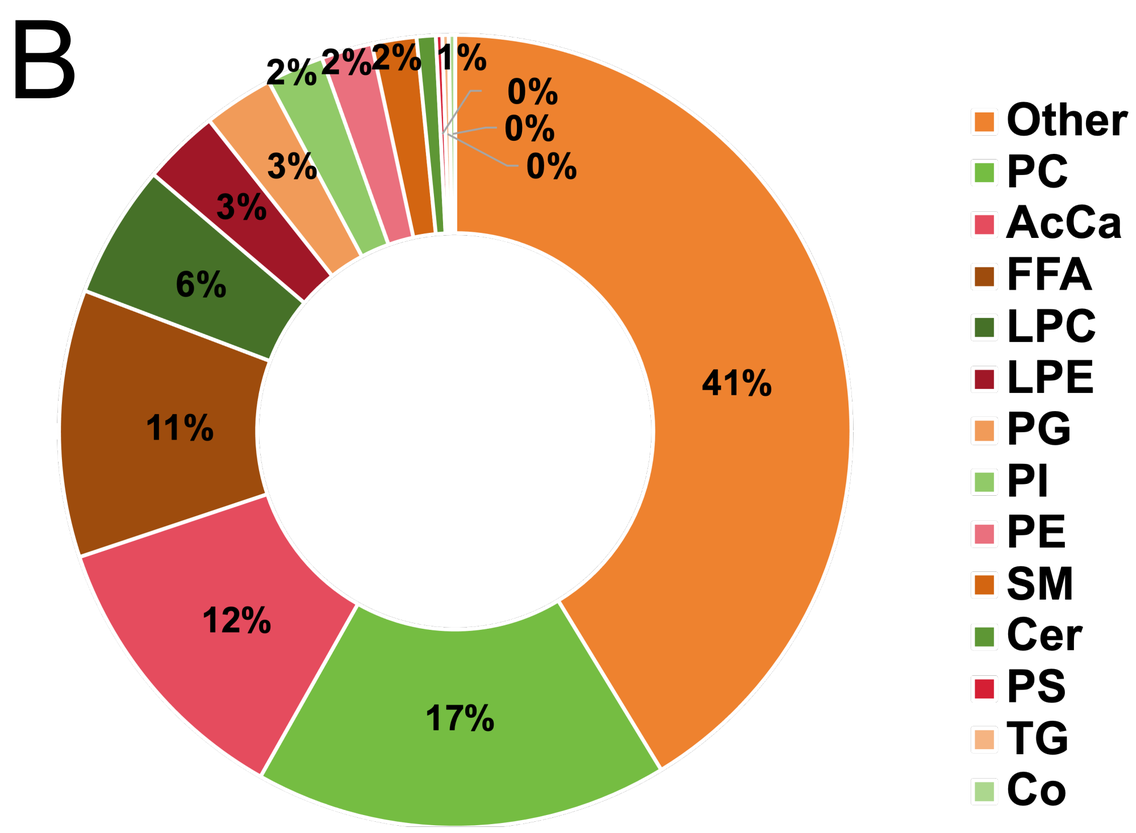
41%
17%
12%
11%
6%
3%
3%
2%
2%
2%
1%
0%
0%
0%
Other
PC
AcCa
FFA
LPC
LPE
PG
PI
PE
SM
Cer
PS
TG
Co

C

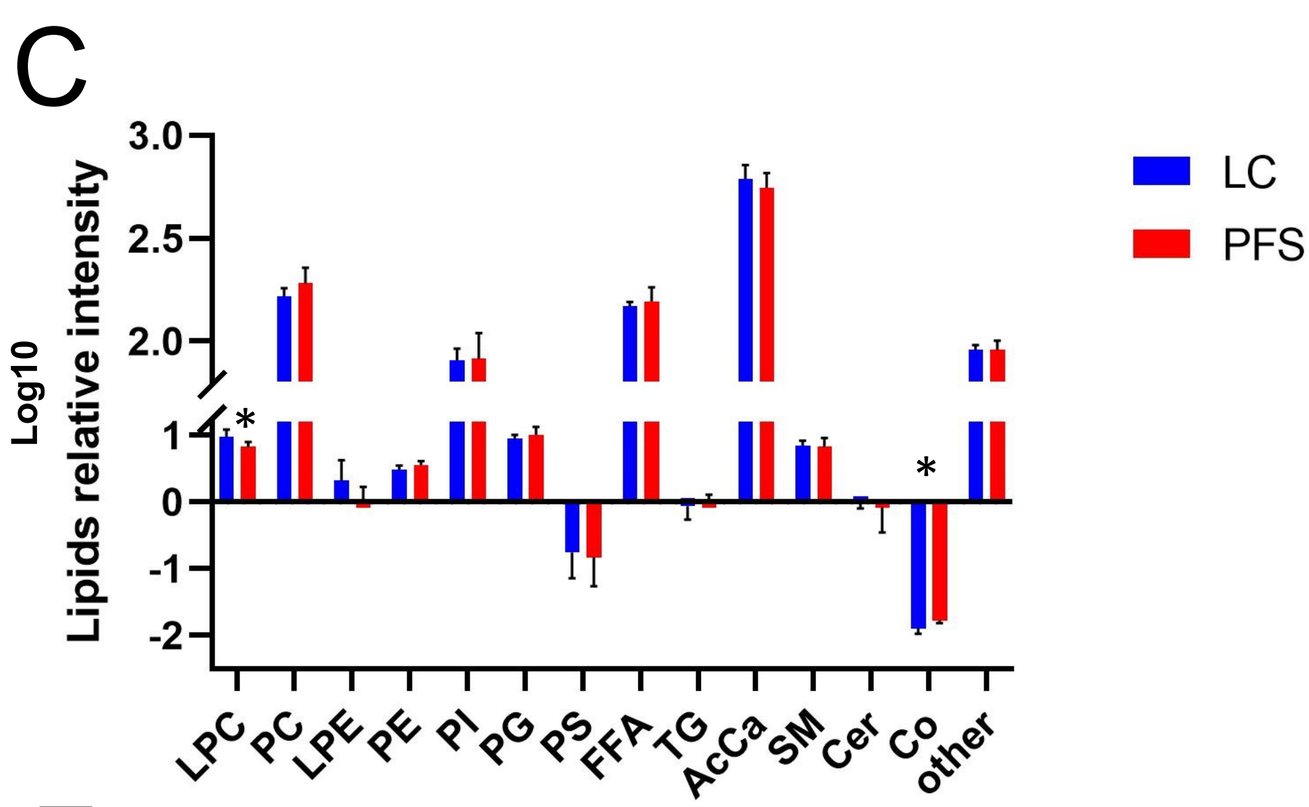
Log10
Lipids relative intensity
3.0
2.5
2.0
1
0
-1
-2
*
*
LC
PFS
LPC
PC
LPE
PE
PI
PG
PS
FFA
TG
AcCa
SM
Cer
Co
other

D

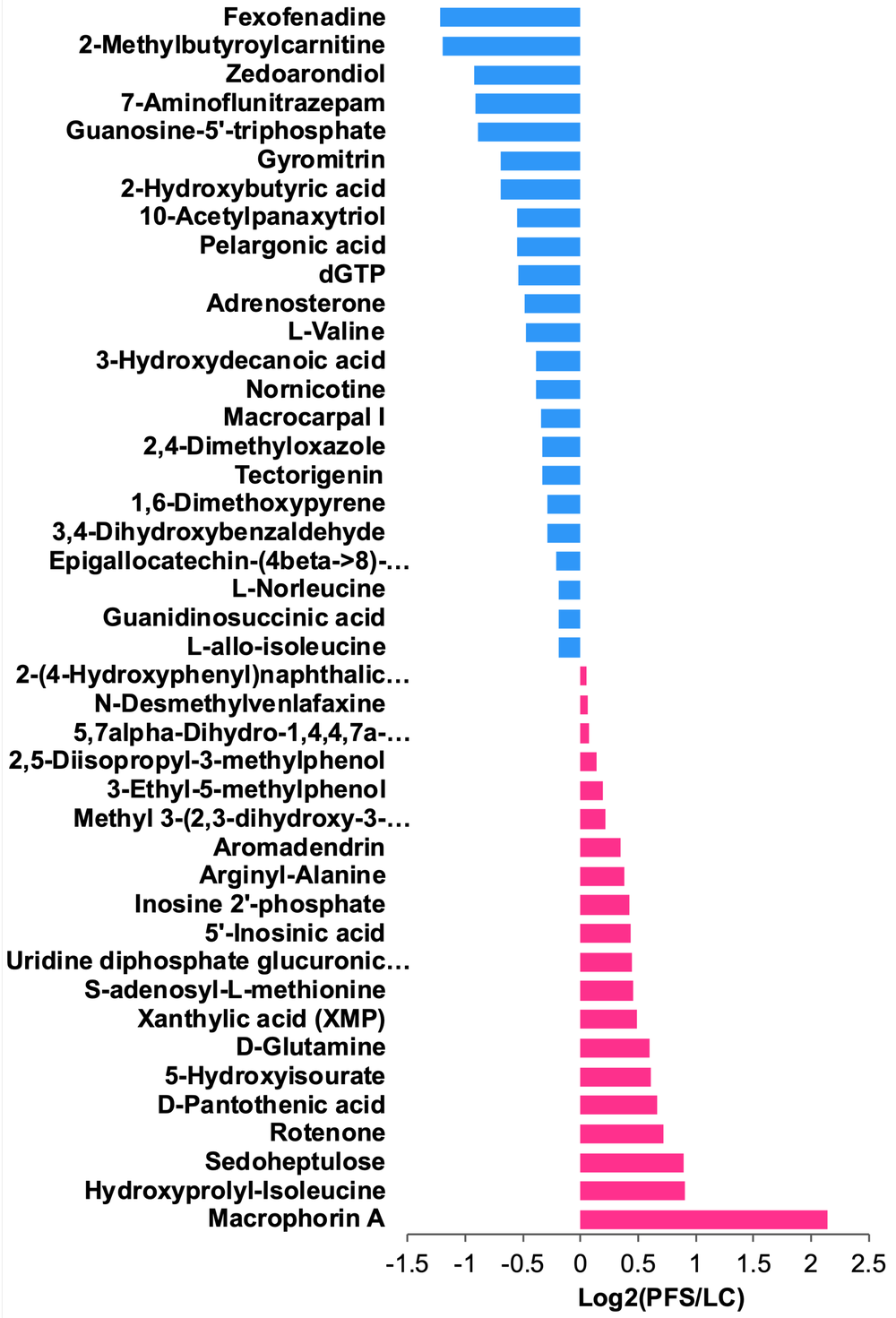
Fexofenadine
2-Methylbutyroylcarnitine
Zedoarondiol
7-Aminoflunitrazepam
Guanosine-5'-triphosphate
Gyromitrin
2-Hydroxybutyric acid
10-Acetylpanaxytriol
Pelargonic acid
dGTP
Adrenosterone
L-Valine
3-Hydroxydecanoic acid
Nornicotine
Macrocarpal I
2,4-Dimethyloxazole
Tectorigenin
1,6-Dimethoxypyrene
3,4-Dihydroxybenzaldehyde
Epigallocatechin-(4beta->8)-...
L-Norleucine
Guanidinosuccinic acid
L-allo-isoleucine
2-(4-Hydroxyphenyl)naphthalic...
N-Desmethylvenlafaxine
5,7alpha-Dihydro-1,4,4,7a-...
2,5-Diisopropyl-3-methylphenol
3-Ethyl-5-methylphenol
Methyl 3-(2,3-dihydroxy-3-...
Aromadendrin
Arginyl-Alanine
Inosine 2'-phosphate
5'-Inosinic acid
Uridine diphosphate glucuronic...
S-adenosyl-L-methionine
Xanthylic acid (XMP)
D-Glutamine
5-Hydroxyisourate
D-Pantothenic acid
Rotenone
Sedoheptulose
Hydroxyprolyl-Isoleucine
Macrophorin A
-1.5
-1
-0.5
0
0.5
1
1.5
2
2.5
Log2(PFS/LC)

E

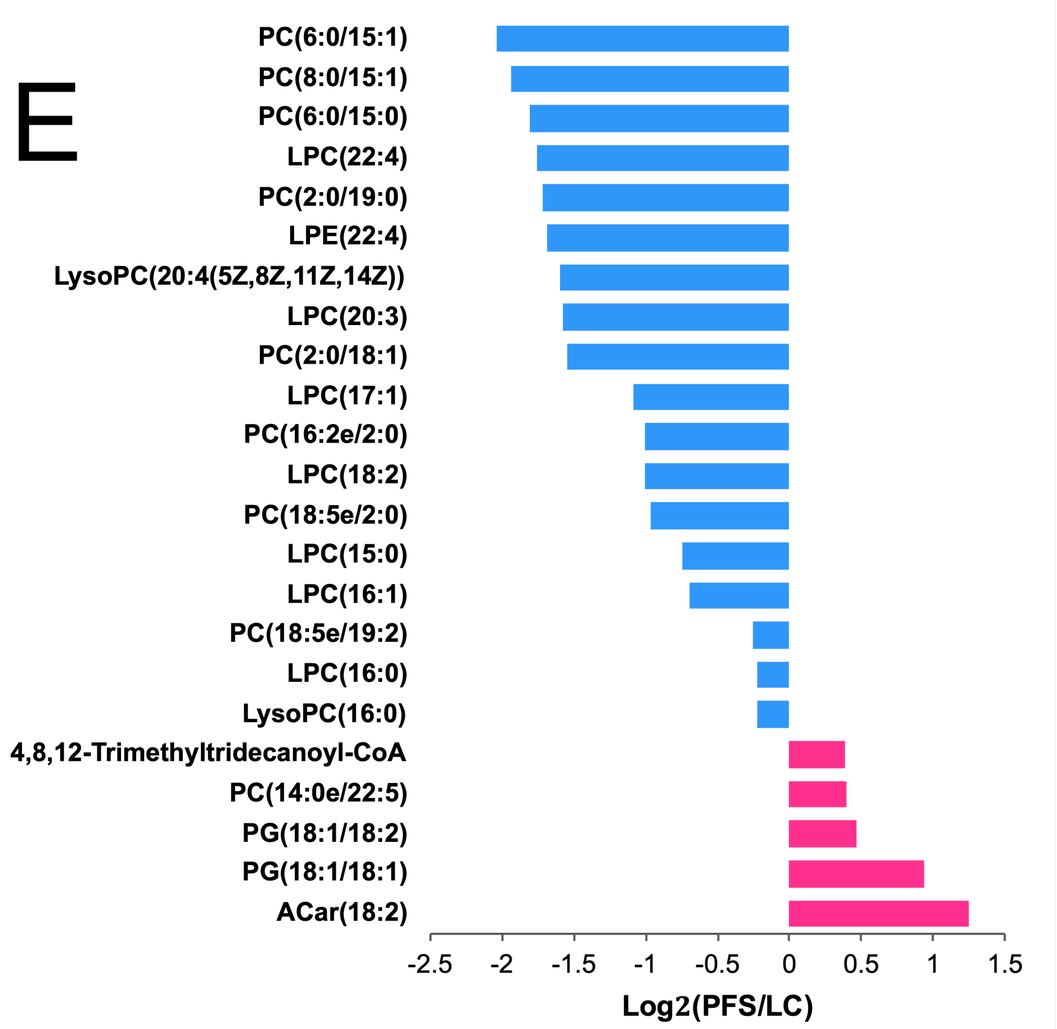
PC(6:0/15:1)
PC(8:0/15:1)
PC(6:0/15:0)
LPC(22:4)
PC(2:0/19:0)
LPE(22:4)
LysoPC(20:4(5Z,8Z,11Z,14Z))
LPC(20:3)
PC(2:0/18:1)
LPC(17:1)
PC(16:2e/2:0)
LPC(18:2)
PC(18:5e/2:0)
LPC(15:0)
LPC(16:1)
PC(18:5e/19:2)
LPC(16:0)
LysoPC(16:0)
4,8,12-Trimethyltridecanoyl-CoA
PC(14:0e/22:5)
PG(18:1/18:2)
PG(18:1/18:1)
ACar(18:2)
-2.5
-2
-1.5
-1
-0.5
0
0.5
1
1.5
Log2(PFS/LC)

F

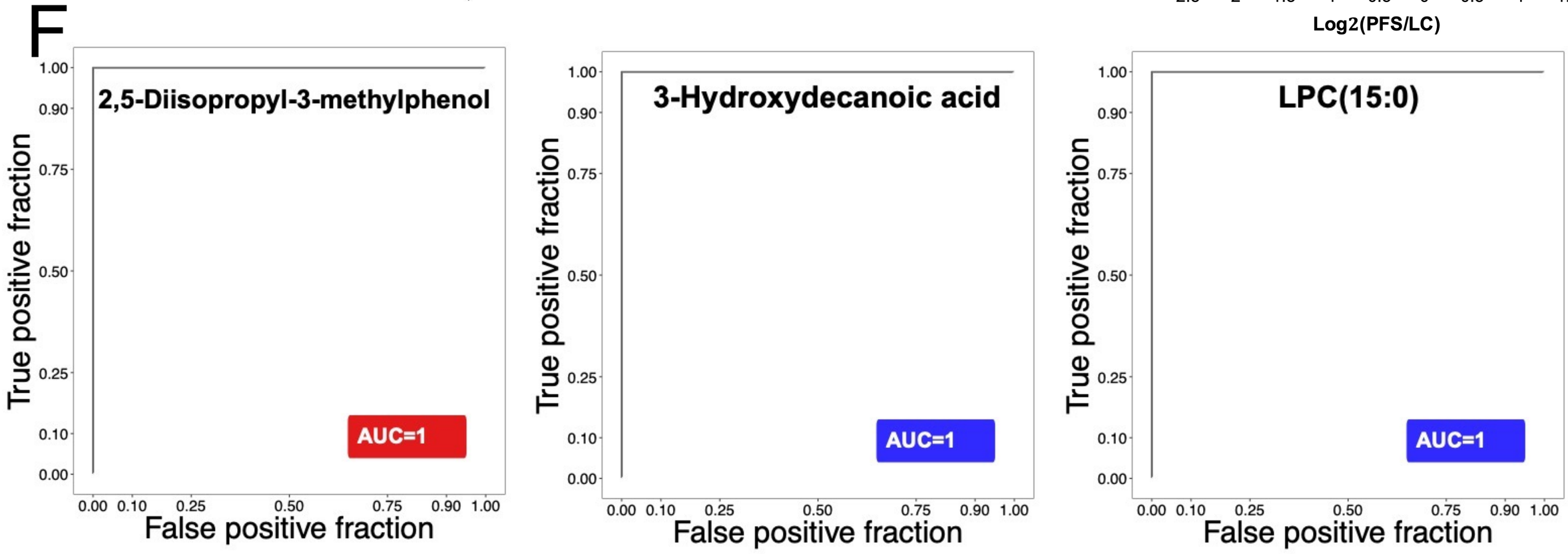
2,5-Diisopropyl-3-methylphenol
AUC=1
3-Hydroxydecanoic acid
AUC=1
LPC(15:0)
AUC=1
True positive fraction
False positive fraction
0.00
0.10
0.25
0.50
0.75
0.90
1.00

A

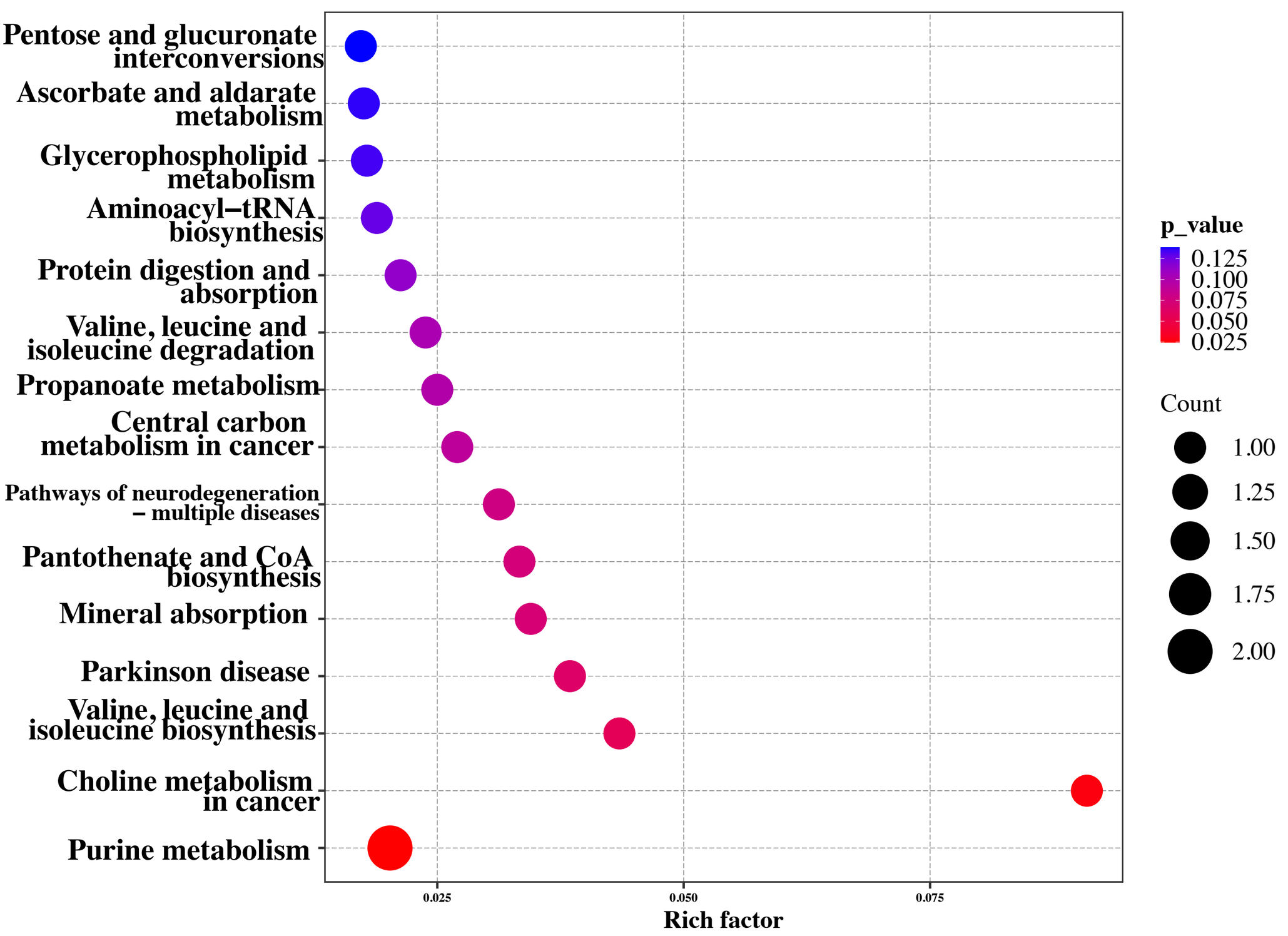
Pentose and glucuronate interconversions
Ascorbate and aldarate metabolism
Glycerophospholipid metabolism
Aminoacyl−tRNA biosynthesis
Protein digestion and absorption
Valine, leucine and isoleucine degradation
Propanoate metabolism
Central carbon metabolism in cancer
Pathways of neurodegeneration − multiple diseases
Pantothenate and CoA biosynthesis
Mineral absorption
Parkinson disease
Valine, leucine and isoleucine biosynthesis
Choline metabolism in cancer
Purine metabolism
0.025
0.050
0.075
Rich factor
p_value
0.125
0.100
0.075
0.050
0.025
Count
1.00
1.25
1.50
1.75
2.00

B

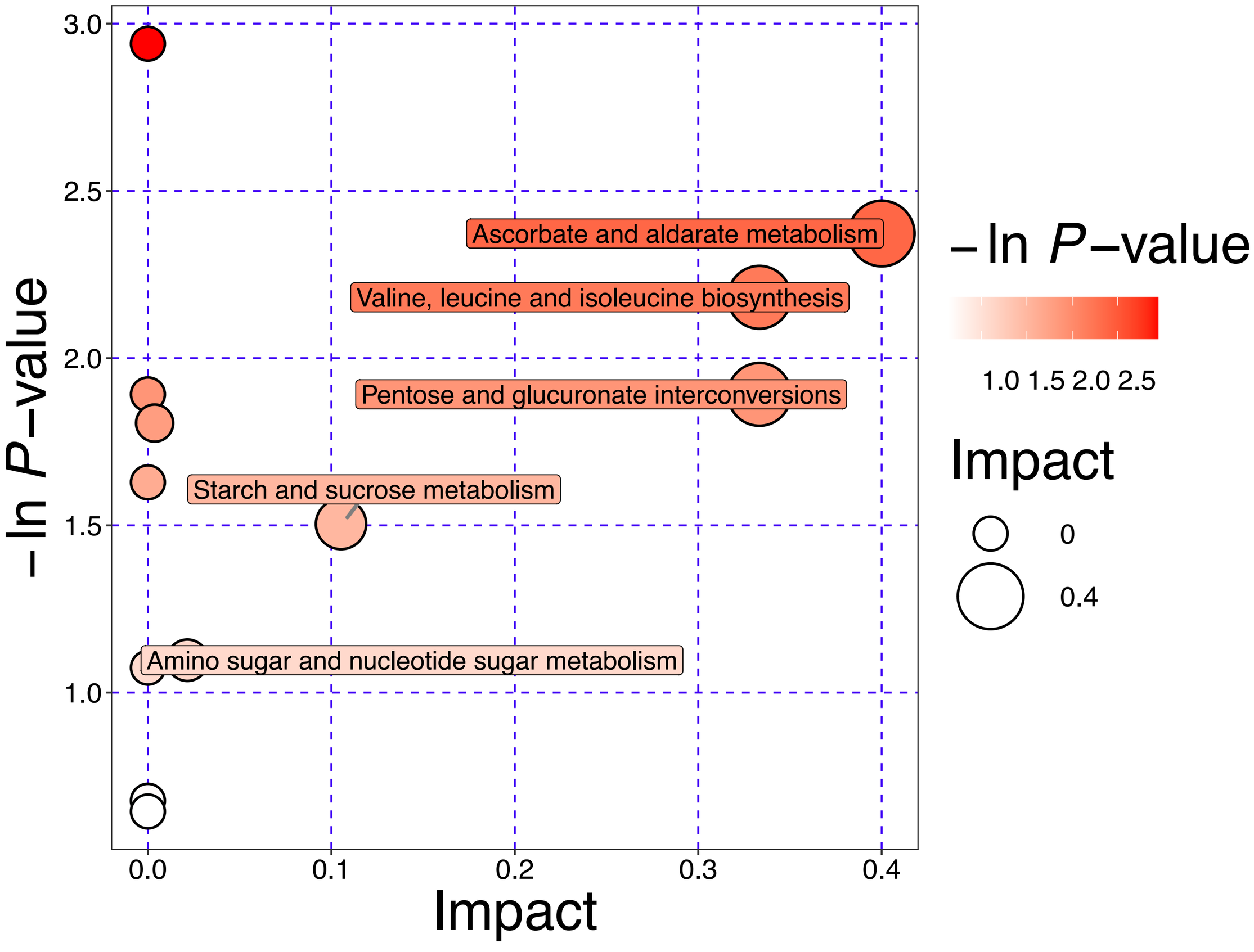
3.0
2.5
2.0
1.5
1.0
−ln P−value
Ascorbate and aldarate metabolism
Valine, leucine and isoleucine biosynthesis
Pentose and glucuronate interconversions
Starch and sucrose metabolism
Amino sugar and nucleotide sugar metabolism
0.0
0.1
0.2
0.3
0.4
Impact
−ln P−value
1.0 1.5 2.0 2.5
Impact
0
0.4

Exploring the metabolomic landscape: *Perilla frutescens* as a promising enhancer of production, flavor, and nutrition in Tan lamb meat

Yue Yu[a], Boyan Zhang[a], Xianzhe Jiang[a], Yimeng Cui[a], Hailing Luo[a], Sokratis Stergiadis[b], Bing Wang[a,*]

[a]*State Key Laboratory of Animal Nutrition, College of Animal Science and Technology, China Agricultural University, Beijing 100193, P. R. China*

[b]*University of Reading, School of Agriculture, Policy and Development, Department of Animal Sciences, Reading RG6 6EU, United Kingdom*

*Corresponding author: Bing Wang (wangb@cau.edu.cn)

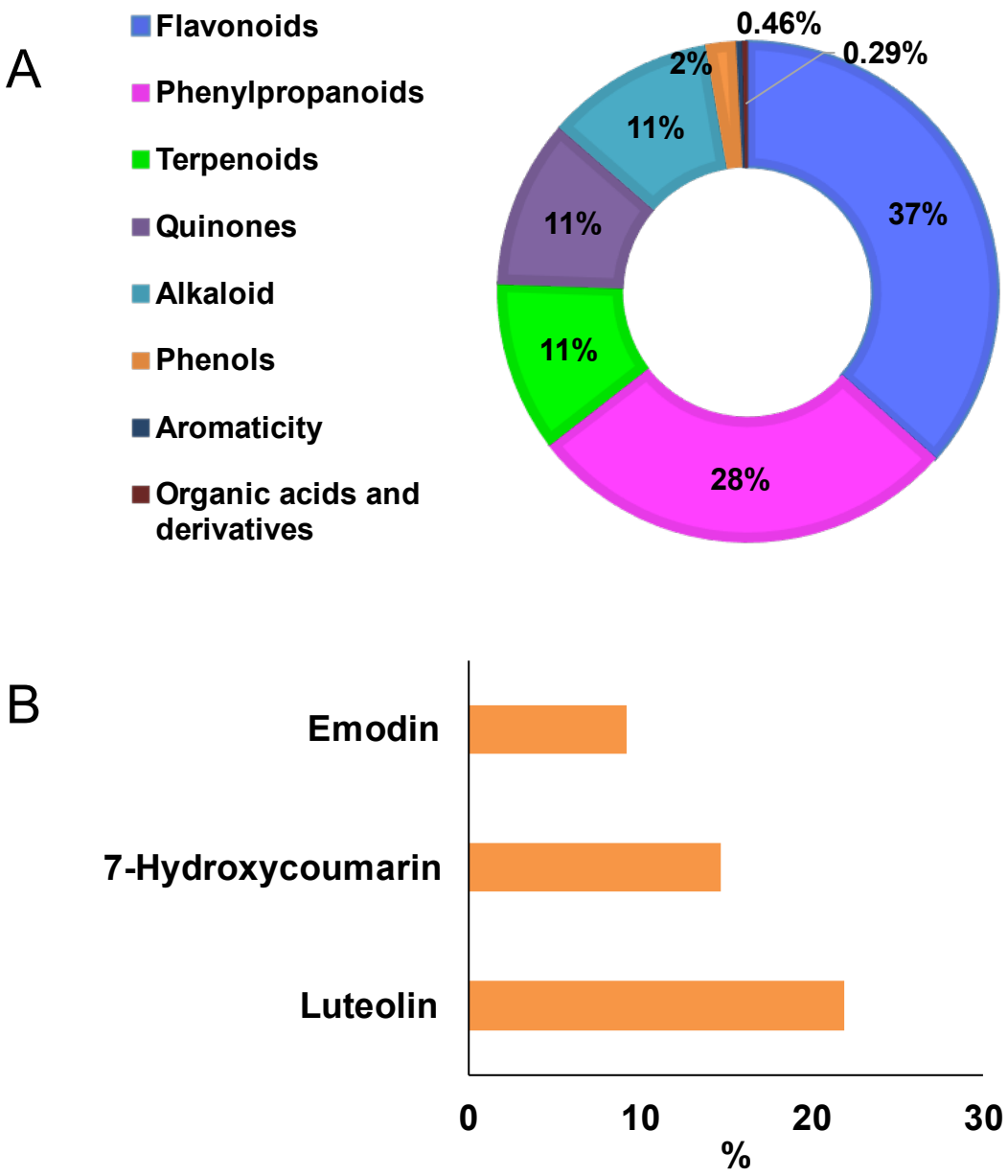

Fig. S1. The plant secondary metabolites of *Perilla Frutescens* seeds. (A) the main categories of plant secondary metabolites. (B) the top three compounds of plant secondary metabolites.

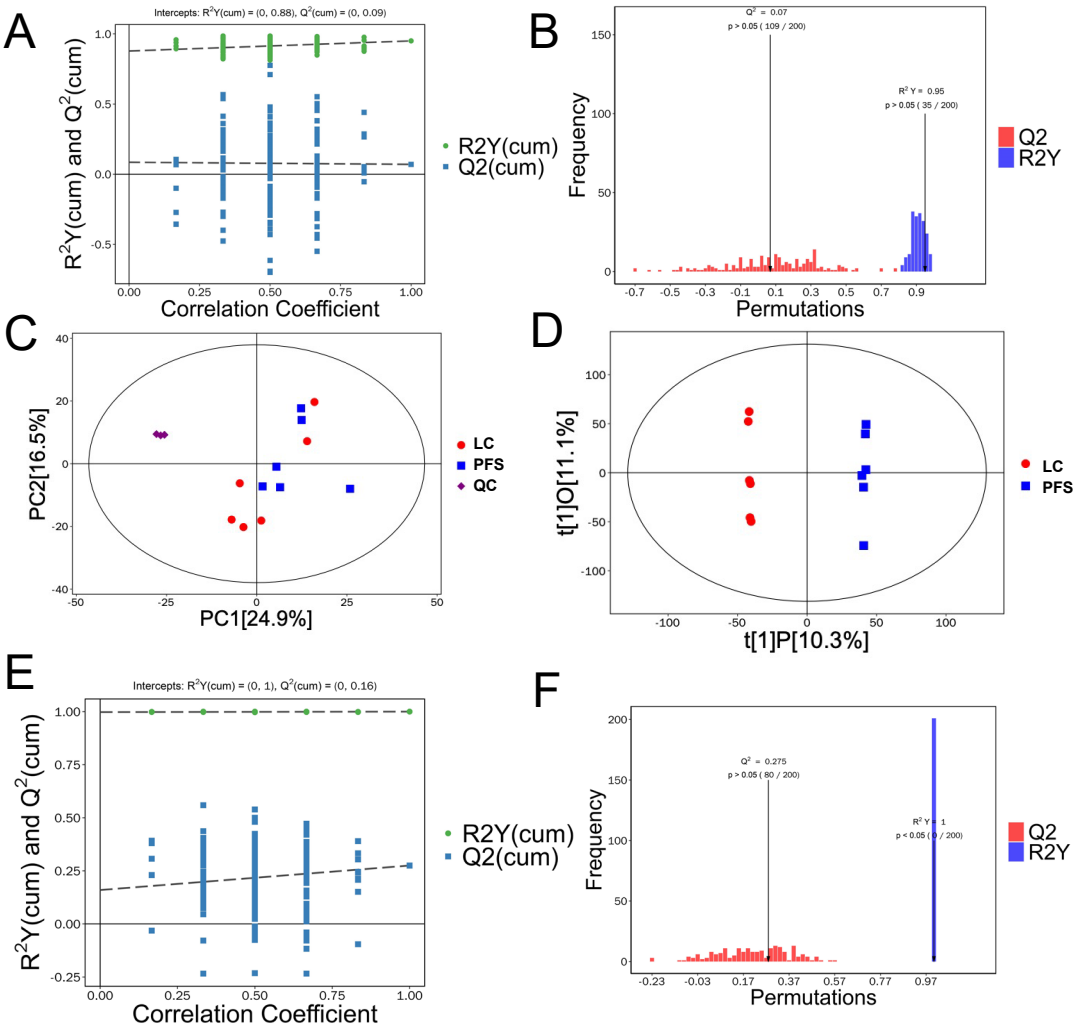

Fig. S2. The principal component analysis (PCA) and supervised orthogonal projections to latent structures-discriminant analysis (OPLS-DA) plots. (A-B) the permutation plot and histogram test of the OPLS-DA model based on GC-MS. (C) PCA score plots of lipophilic and hydrophilic metabolites. (D) OPLS-DA score plots of lipophilic and hydrophilic metabolites. (E-F) the permutation plot and histogram test of the OPLS-DA model based on high-definition mix discovery LC-MS/MS.